FENN COLLEGE OF ENGINEERING
CLEVELAND STATE UNIVERSITY

Electrical Engineering

ERROR ANALYSIS IN THE MEASUREMENT
OF AVERAGE POWER WITH APPLICATION
TO SWITCHING CONTROLLERS

FINAL TECHNICAL REPORT

NASA GRANT NO. 3222

Principal Investigator: James E. Maisel

Period Covered: From 10-1-78 to 10-1-79

Cleveland State University
Cleveland, Ohio   44115

TABLE OF CONTENTS

ERROR ANALYSIS IN THE MEASUREMENT
OF AVERAGE POWER WITH APPLICATION TO
SWITCHING CONTROLLERS

James E. Maisel
Cleveland State University

ABSTRACT

Power measurement errors due to the bandwidth of a power
meter and the sampling of the input voltage and current of a
power meter were investigated assuming sinusoidal excitation
and periodic signals generated by a model of a simple DC/DC
chopper system. Errors incurred in measuring power using a
microcomputer with limited data storage were also considered.

In this investigation, the behavior of the power measure-
ment error due to the frequency responses of first order trans-
fer functions between the input sinusoidal voltage, input sinu-
soidal current and the signal multiplier was studied. Results
indicate that this power measurement error can be minimized if
the frequency responses of the first order transfer functions
are identical.

The power error analysis was extended to include the power
measurement error for a model of a simple DC/DC chopper system
with a DC power source and an ideal shunt motor acting as an
electrical load for the chopper. The behavior of the power
measurement error was determined as a function of the chopper's
duty cycle and back emf of the shunt motor. Results indicate
that the error is large when the duty cycle or back emf is small.

Theoretical and experimental results indicate that the power
measurement error due to sampling of sinusoidal voltages and
currents becomes excessively large when the number of obser-
vation periods approaches one-half the size of the microcomputer
data memory allocated to the storage of either the input sinu-
soidal voltage or current.

I. INTRODUCTION

This report contains a study of power measurement errors
due to the bandwidth and phase mismatch of a power meter and
the sampling of the input voltage and current of a power
measuring instrument [1,2].

The power measurement error due to the frequency response
of a wattmeter is general to all types of wattmeters both
analog and digital. The frequency response of the power
measuring instrument is affected not only by its internal
electrical system but also by the external electrical system
that exists between the voltage and current that is to be moni-
tored. For example, the frequency response and phase shift of
the current shunt and voltage divider which is an integral part
of the power measuring system should be considered when studying
the power measurement error. Even electrical cables connecting
the current shunt and voltage divider to the wattmeter should
be considered as part of the power measuring system if the
electrical cables are appreciable part of a wavelength. Not
only do the cables introduce amplitude and phase distortion but
can introduce time delays between the voltage and current. The
exact behavior of the frequency response will be dependent on
the choice of wattmeter, voltage divider, current shunt, and
the electrical connections.

In order to perform a power error analysis, the response
of these electrical elements must be specified. In this
investigation, it will be assumed that the transfer functions
are first order between the points where the voltage and current
are measured and where the multiplication of the voltage and
current is actually performed. Hence the frequency response
of the transfer functions decreases approximately at the rate
of 20 db/decade beyond the corner frequency of the transfer
function.

If the input voltage and current to the power meter are sampled, another power measurement error is introduced due to sampling. It will be shown that if the number of observed periods of a sinusoidal voltage or current is exactly equal to one-half the size of data memory allocated to the storage of either the input sinusoidal voltage or current, the power measurement error will be so large that the power measurement will be meaningless. This result is based on the assumption that both data memory size and the sampling rate are finite. Under the condition that the number of observed periods is one-half the data memory size, the number of samples per period is exactly two, which is exactly the minimum number of samples required according to Shannon's theorem [3].

The power measurement error due to the bandwidth and sampling cannot be analyzed until the current and voltage waveforms are specified as a function of time. In other words, the behavior of the power measurement error will change with the waveform of the input voltage and current. It can be easily shown if the input voltage and current are assumed periodic functions of time and superposition of harmonic power is·applied, the total average power, P_T, can be represented by summing the harmonic average power, P_n

$$P_T = \sum_{n=0}^{\infty} P_n . \tag{1}$$

The normalized error of the total power is related to the normalized error of the nth harmonic average power and assumes the form

$$\Delta P_T / P_T = \sum_{n=0}^{\infty} (P_n / P_T)(\Delta P_n / P_n) . \tag{2}$$

Note that the normalized error of the nth harmonic average power is multiplied by a weighting factor, P_N / P_T. In order to determine this weighting factor, the waveform of the voltage and current

must be specified. In this study of power measurement error, two waveforms will be used; they are: the sinusoidal signal and the waveforms generated by a simplified DC/DC chopper system.

The power error analysis using a single frequency approach offers the advantage of studying the behavior of the power measurement error using trigonometric equations which can be manipulated into mathematical forms that are easily understood. The results of the single frequency error analysis can be extended to more than one frequency, but the error analysis becomes more complex.

The waveforms generated by a simple DC/DC chopper system offer the other extreme in error analysis when a complete Fourier analysis has to be performed in order to study the behavior of the power measurement error. The choice of simple DC/DC chopper system was based on the fact that such a system is used to control large amounts of power such as in an electric vehicle. Since electric vehicle's efficiency is very important from a practical viewpoint, an understanding of the power measurement error as a function of system parameters has a very high priority if the vehicle's driving range is to be optimized.

This study also investigates the feasibility of using a microcomputer as a wattmeter. The results of the investigation show that if the number of periods observed by the microcomputer approaches half the data memory alloted to either voltage or current, the microcomputer's output has a large power measurement error. This is due to the fact that the microcomputer samples the input signals at a finite rate.

II. ELECTRICAL MODEL OF A PHYSICAL WATTMETER

The power delivered to an electrical system as a function of time is given by the product of the instantaneous voltage and current at the input terminals to the electrical system. Since the voltage and current will in general vary from instant to instant, the product of instantaneous voltage and current will also be a function of time. This product is defined as instantaneous power,

$$p(t) = e(t)\, i(t) \qquad (3)$$

where e and i are the instantaneous voltage and current. The average value of the instantaneous power or total average power is defined as

$$P_T = \frac{1}{t_2 - t_1} \int_{t_1}^{t_2} p(t)dt \qquad (4)$$

where t_1 and t_2 represents the beginning and end of an observation time. Since no restriction is placed on either the instantaneous voltage or current, the average power will in general be dependent on the length of observation time.

If the instantaneous voltage and current are periodic, the total average power is

$$P_T = \frac{1}{T_P} \int_0^{T_P} p(t)dt \qquad (5)$$

where T_P is the period. For the general case where voltage and current are periodic, Equation (5) can be used to calculate total average power providing that T_P represents the time of the fundamental period.

Employing Fourier series analysis to a periodic voltage and current, the complex waveforms can be expressed in terms of an average component and an infinite sum of cosine functions.

The general trigonmetric form for the Fourier series [4] is

$$e(t) = V_o + \sum_{n=1}^{\infty} V_n \cos (n\omega_o t + \psi_n) \qquad (6\text{-}a)$$

$$i(t) = I_o + \sum_{n=1}^{\infty} I_n \cos (n\omega_o t + \phi_n) \qquad (6\text{-}b)$$

where V_o and I_o represent the average value of $e(t)$ and $i(t)$ respectively; V_n, ψ_n and I_n, ϕ_n represent the magnitude and phase angle of the nth harmonic of voltage and current, respectively; and ω_o represents the fundamental angular frequency $(\omega_o = 2\pi/T_p)$.

Using Parseval's theorem [5], it can be shown that the total average power for a general periodic signal can be expressed as an infinite sum of harmonic average powers. The result is

$$P_T = V_o I_o + \tfrac{1}{2} \sum_{n=1}^{\infty} V_n I_n \cos (\psi_n - \phi_n) . \qquad (7)$$

Equation (7) relates the harmonic average power content of a periodic signal to the total average power. Note that for the nth harmonic both V_n and I_n could be large in magnitude and still the average power associated with the nth harmonic would be zero if $\psi_n - \phi_n = \pm 90^o$. This point will be emphasized in a later section.

Although the above equations may describe an ideal power meter, physical wattmeters deviate from the ideal case because the power instrument will measure quantities that are proportional to input voltage and current. If the proportionality constants are known, they can be accounted for in the design of the wattmeter so that the instrument reads the correct value at any frequency.

A more general approach to modeling a wattmeter is shown in Figure 1. The transfer functions from the respective voltage and current inputs to the multiplier account for any electrical networks that exist between the inputs of the power meter and multiplier. For example, a current shunt could be considered

a part of H_I and a voltage divider could be included in the
description of H_V. Besides the external networks such as the
current shunt and voltage dividers, internal electrical net-
works to the multiplier must also be considered as part of
H_I and H_V. For purpose of analysis, it is assumed that the
transfer functions describe first order systems that can be
represented by

$$H_V = 1/(1 + (jn\omega_0)/\omega_1) \qquad (8\text{-}a)$$

$$H_I = 1/(1 + (jkn\omega_0)/\omega_1) \qquad (8\text{-}b)$$

where ω_1 represents the angular frequency where the magnitude
of H_V is 3db down from the mid-band gain. This angular fre-
quency is sometimes referred to as the 3db angular corner fre-
quency or just corner frequency. The parameter k allows the
two transfer functions to have different corner frequencies.
The factor $n\omega_0$ represents the set of discrete angular fre-
quencies associated with nonsinusoidal periodic signals as
determined from the Fourier series.

Since the transfer functions have magnitudes and phase
angles, both quantities will affect the measurement of the
n^{th} harmonic average power. Equation (7) can be modified to
account for the affects of H_V and H_I on the measurement of
total average power. Since H_V and H_I affect the magnitude and
the phase of the nth harmonic of voltage and current, re-
spectively, the approximate total average power [6] which
will be indicated by the power meter is

$$P_{APP} = V_0 I_0 + \tfrac{1}{2} \sum_{n=1}^{\infty} \frac{V_n I_n \cos(\psi_n - \phi_n + \tan^{-1}(n\omega_0/\omega_1) - \tan^{-1}(kn\omega_0/\omega_1))}{((1+(n\omega_0/\omega_1)^2)(1+(kn\omega_0/\omega_1)^2))^{\frac{1}{2}}} \qquad (9)$$

Equation (9) shows that as long as ω_1 is finite, there will
be an error in the measurement of power because the results

predicted by Equation (9) will be different from the results
predicted by Equation (7). The magnitudes of the transfer
functions affect the product of $V_n I_n$ while the corresponding
transfer function phase angles affect the resultant power
phase angle. If k=1, the resultant power phase angle is in-
·dependent of ω because the two arc tangent expressions in
Equation (9) cancel each other. In this case, only the
magnitude of the transfer functions introduce an error in the
measurement of average power. As the bandwidth of the instru-
ment decreases ($\omega_1 \rightarrow \omega_0$), the power measurement error will
correspondingly increase until errors are so large that a
power measurement will have little or no meaning.

If the input signals to the wattmeter are periodic,
the bandwidth of the wattmeter should be large enough to en-
compass all the important power contributing harmonic com-
ponents in order to minimize the power measurement error.
Section III will develop the relationships between bandwidth
of a wattmeter and the corresponding power measurement error
for a specific set of periodic signals.

III. ERROR ANALYSIS IN THE MEASUREMENT OF AVERAGE
POWER OF SINUSOIDAL SIGNALS

This part of the report will primarily be devoted to
the error analysis in the measurement of average power of
sinusoidal signals. Although single frequency power error
analysis is somewhat restrictive, it does offer a clear view
about the power error behavior. The results can be extended
to include the non-sinusoidal periodic case if the true
harmonic power content is known.

A. Power Measurement Error Due to Transfer Functions H_V and H_I

As discussed in Section I, the two transfer functions H_V
and H_I affect wattmeter accuracy especially when the wattmeter's
bandwidth is of the same order as the highest important harmonic.
The actual distribution of harmonic power will not only depend
on the amplitudes of the harmonic voltage and current, but
also on the phase relationship between the voltage and current.
Thus, the distribution of harmonic power will depend strongly
on the profile of instantaneous voltage and current in the
time domain. Since there are an infinite number of voltage
and current profiles, the error analysis does not lend itself
to a closed form analysis unless specific profiles are chosen
for the instantaneous voltage and current. A sinusoidal wave-
form offers the simplest approach because the power equations
can be expressed in closed form through the superposition of the
power theorem, the results can be extended to more complex
periodic signals. Because Equation (9) is general for any
periodic waveform, one term out of the infinite set of power
terms can be used to represent the sinusoidal profile and is
given by

$$P_{APP} = ((V_m I_m/2)/((1+x^2)(1+(kx)^2))^{\frac{1}{2}})(\cos(\theta+\tan^{-1}(x)-\tan^{-1}(kx))) \quad (10)$$

where V_m and I_m represent the amplitude of the sinusoidal voltage

and current, respectively; x represents the normalized angular
frequency $(x = \omega/\omega_1)$; and θ represents the phase angle between
the voltage and current. The parameter k has the same meaning
as in Euqation (8). The true average power is given by the
relationship

$$P_T = \lim_{\substack{\omega_1 \to \infty \\ k \text{ finite}}} P_{APP} = (V_m I_m/2)\cos\theta. \tag{11}$$

If Equation (10) is divided by Equation (11), the re-
sultant function will be independent of the peak voltage and
current and a function of x,k, and θ only. The ratio P_{APP}/P_T
is defined as the normalized correction factor, NCF. The true
average power P_T is equal to P_{APP}/NCF. Therefore, it is
important that NCF be as near to unity as possible for
accurate power measurements. The normalized correction factor
NCF is given by

$$NCF = (1/((1+x^2)(1+(kx)^2))^{\frac{1}{2}})(\cos(\theta+\tan^{-1}(x)-\tan^{-1}(kx))/\cos\theta). \tag{12}$$

In general, NCF will approach $\pm \infty$ as the phase angle approaches
$\pm90^o$, respectively, providing x is not zero. Hence the
power measurement becomes meaningless for very small power
factors if $\tan^{-1}x - \tan^{-1}(kx) \neq 0$. Equation (12) shows that
if k is equal to unity, NCF will be independent of the phase
angle. By carefully matching the frequency response of H_V
and H_I, (k=1), Equation (12) will be a function of the normalized
frequency x, only.

Figures 2, 3, and 4 show the behavior of the correction
factor as a function of the normalized frequency with k and
θ as parameters. Except for the case where k=1, the correction
factor, NCF, is strongly dependent upon the phase angle and
becomes more pronounced as the power factor approaches zero.

According to Equation (12), the correction factor should display some sort of oscillatory behavior as a function of the normalized frequency, with oscillations becoming more pronounced at low power factors. The normalized frequency in Figures 2, 3., and 4 is restricted between zero and unity. Above unity the normalized frequency implies that the actual frequency exceeds the bandwidth of either H_V of H_I; this is not the normal frequency range for the power meter. Although Figures 2 and 3 are informative, they are not very useful from a measurement viewpoint because the correction factor varies over too large a range for meaningful results. By restricting the range of the normalized frequency (see Figure 4), a tighter correction factor tolerance ($0.98 \leq$ NCF ≤ 1.02) can be achieved. This, of course, restricts the useful frequency range of H_V and H_I.

It is obvious from Figure 2 that H_V and H_I should have identical frequency responses (k=1) if the correction factor is to be independent of the phase angle. For $x \rightarrow 0$, NCF $\rightarrow 1$ regardless of the values of k and θ. For $k = 1 + \Delta k$, which allows for slight differences in the frequency response between H_V and H_I, a linear equation representing NCF as a function of x, assuming $x \rightarrow 0$ with θ and Δk treated as parameters, can be derived indirectly from Equation (12) by expressing Equation (12) as a fourth order polynominal. The polynominal is given by

$$(NCF)k^2x^4 + ((NCF)(1+k^2)-k)x^2 + ((1-k)\tan\theta)x + NCF-1 = 0 . \tag{13}$$

For the case $k = 1 + \Delta k$, $x \rightarrow 0$, NCF $\rightarrow 1$, Equation (13) is reduced to the linear equation

$$NCF = 1 - (\Delta k \tan\theta)x . \tag{14}$$

The slope, $\Delta k \tan\theta$, becomes very large in magnitude as the power factor angle approaches $\pm 90^\circ$ for $\Delta k \neq 0$, and is positive for θ negative and negative for θ positive. The result is consistent with Figures 2, 3, and 4.

For the case where the voltage and current are periodic functions of time, the true total power can be expressed as a function of approximate harmonic power and the corresponding NCF_n by

$$P_T = \sum_{n=0}^{\infty} P_{APP_n}/NCF_n. \tag{15}$$

Although Equation (15) gives the same results as Equation (7), the form of Equation (15) is such that each approximate n^{th} harmonic power must be known or measured and the corresponding n^{th} harmonic phase angle be known or measured in order to determine NCF_n for the corresponding n^{th} harmonic. However, Equation (15) does emphasize that a wattmeter having a small power measurement error must have NCF_n as close to unity as possible with a correspondingly small normalized frequency. This can be accomplished using a wattmeter which has a bandwidth much broader than the important harmonics contained in the voltage and current signal and one which has identical frequency responses for H_V and H_I (k=1). If the bandwidth of the wattmeter is many times larger than the important harmonics being monitored by the wattmeter, the frequency matching of the two transfer functions, H_V and H_I can be re-laxed to some degree.

B. Power Measurement Error Due to Sampling the Voltage and Current

This portion of the report will primarily be concerned with power measurement error analysis associated with sampling voltage and current and the determination of total average power based on these samples. For example, this type of power measurement error occurs when a microcomputer is used as a power meter; the input analog signals are sampled, con-verted to digits, stored, and manipulated to generate an output equal to the average power. In order to develop a

power error equation in closed form, it will be assumed
that the input voltage and current are sinusoidal.

Before investigating the behavior of power measure-
ment error due to sampling, it is instructive to first ex-
plore the power measurement error associated with continuous
signals. This would be equivalent to sampling at an infinite
rate with a power computing system having an infinite memory.
Instantaneous power can be expressed as

$$p(t) = (V_m I_m/2)(\cos\theta - \cos(2\omega t + \theta)). \qquad (16)$$

Using Equation (4) for the definition of average power and
letting $t_2 - t_1 = T_0$, the observation time interval, the approxi-
mate average power due to the finite T_0 is

$$\tilde{P} = (V_m I_m/2)\cos\theta - ((V_m I_m T_P)/(8\pi T_0))(\sin(4\pi T_0/T_P + \theta) - \sin\theta) \qquad (17)$$

where $T_P = 2\pi/\omega$. The true average power is given by the first
term in Equation (17). The second term can be interpreted
as an error term which oscillates with a period $T_P/2$ and de-
creases as the observation time, T_0, becomes large with re-
spect to the period T_P. The normalized power error, NPE, is
defined in terms of true average power,

$$NPE = (P - \tilde{P})/P_T = (\sin(4\pi C + \theta) - \sin\theta)/(4\pi C \cos\theta) \qquad (18)$$

where $C = T_0/T_P$, the number of periods or partial periods
that are observed in time T_0. The normalized power error is
a decreasing oscillatory function of period C and is zero
for multiples of C/2. For a given C (C not equal to a
multiple of ½), NPE approaches $\pm\infty$ as θ approaches $\pm90^\circ$.
Using L'Hospital's Rule, it can be shown that if C is equal

to a multiple of ½, NPE approaches zero even as θ approaches $\pm90^{o}$.

It can be concluded from the above discussion that a wattmeter capable of observing C periods equal to a multiple of ½ periods, the NPE will be zero for any value of θ. If C is other than a multiple of ½ periods, NPE is not zero and there will be a difference between the true average power and approximate average power. This power error is usually small when using a conventional laboratory wattmeter because the observation time is usually much greater than the period of the signal (human response time must be considered) being monitored by the wattmeter. However, a microcomputer, with a very large memory but finite sampling interval could be programmed to determine the approximate average power over an observation time interval comparable to the period of the input voltage and current. The value of NPE could become significant, especially if the phase angle approaches $\pm90^{o}$.

If the input voltage and current are sampled at a finite rate and the memory size is finite, the above results for the continuous case are no longer valid in a strict sense. The normalized power error no longer keeps on decreasing with increasing C because of the finite sampling rate and finite data memory size. This condition is observed when a microcomputer with finite data storage capability is programmed to function as a wattmeter. The analog input signals are sampled and processed to obtain the approximate average power. The gating time or observation time will depend on the memory size and time between samples and is given by

$$T_o = NT_s \tag{19}$$

where N represents data memory size and T_s the time between samples. For a given data memory size, the observation time is proportional to the sampling time interval. For large

sampling frequencies (T_s is small) it is possible for T_o to become comparable to the period of the input signals thus causing the power measurement error to be excessive.

The discrete form of Equation (16) can be written

$$p(nT_s) = (V_m I_m/2)(\cos \theta - \cos (4\pi nT_s/T_P + \theta)). \tag{20}$$

The corresponding approximate average power is found by summing Equation (20) over memory size N. $\tilde{P}$ is given by

$$\tilde{P} = (1/(N+1)) \sum_{n=0}^{N} p(nT_s). \tag{21}$$

It is convenient to define a power measurement error similar to Equation (18) except that it will be called the normalized sampled power error, NSPE. The result is

$$NSPE = 1 - \tilde{P}/P = (1/(N+1))(\sum_{n=0}^{N} \cos(4\pi nT_s/T_P+\theta)/\cos\theta). \tag{22}$$

Expressing the cosine function in terms of exponentials, and recognizing that the exponential summation is a geometric series, the normalized sampled power error can be expressed in term of periods or fractional periods C. The result is

$$NSPE = (1/(2(N+1)\cos \theta \sin(2\pi C/N)))(\cos(\theta+\psi)-\cos(\theta+\psi+4\pi C)) \tag{23-a}$$

$$\psi = \tan^{-1}(\sin(4\pi C/N)/(2\sin^2(2\pi C/N))). \tag{23-b}$$

If N is allowed to approach infinity,

$$\psi \to \pi/2$$

$$\cos(\theta+\psi) \to -\sin\theta$$

$$\cos(\theta+ +4\pi C) \to -\sin(\theta+4\pi C)$$

$$\sin(2\pi C/N) \to 2\pi C/N.$$

The result is exactly the same as for the continuous case (Equation (18)). If C is chosen to be a multiple of ½, NSPE is zero. This is also consistent with the continuous case.

The major difference between Equations (23-a) and (18) is the factor $\sin(2\pi C/N)$ instead of $4\pi C$. The sine function is cyclic and appears in Equation (23-a) because the input signals are being sampled at a finite rate and the memory size is finite. For a specified N (memory size) and $N \gg 1$, the NSPE will approach +1 and -1 as C approaches 0 and N/2, respectively. The case for C approaching 0 implies that the observation time as well as the sampling time is approaching zero (Equation (19)). This means $\tilde{P}/P$ is approaching zero in the limit or NSPE is a +1 (Equation 22)). As C approaches N/2, the number of samples per period, N/C, approaches 2. The angle ψ (Equation 23-b) approaches $\pi/2$ and NSPE (Equation 23-a) becomes indeterminant. Using L'Hospital's Rule, it can be shown that NSPE $\rightarrow -1$ as $C \rightarrow N/2$.

If C in Equation (23) is replaced by $C_n + \Delta C$, where C_n is an integer, the behavior of NSPE can be studied within a given period C_n. It is assumed that the scanning parameter, ΔC, is restricted to a range from zero to unity. This procedure permits the comparison of NSPE of one period with another period as shown in Figure 5 and 6. Figure 5 shows the behavior of NSPE for $C_n = 1$ and $C_n = 255$ assuming N = 512 and $\theta = 30^\circ$. The plot shows for $C_n = 1$ that the NSPE will reach a maximum of approximately 0.04 and a minimun of approximately -0.10 for ΔC equal to approximately 0.10 and 0.35, respectively. If the power instrument observation time happens to coincide with C = 1.15, or C = 1.35, the power measurement error would be too large for meaningful measurements. For the period 255, which is just before the period where C equals 512/2, the NSPE begins to increase because of the $\sin(2\pi C/N)$ factor in Equation (23-a). Note that NSPE for C = 255 is read along the right hand side of the vertical axis in Figure 5.

Again, the power measurement could be meaningless if the observation time is chosen incorrectly. In both cases, the phase angle was fixed at 30°.

Between $C_n = 0$ and $C_n = 256$, NSPE decreases because the $\sin(2\pi C/N)$ factor in Equation (23-a) is increasing in value. Figure 6 shows the behavior of NSPE for $C_n = 50$, 100, and 127; $\theta = 30^{\circ}$; and $N = 512$. Note that the NSPE is considerably less than for $C_n = 1$ and 255. According to Figure 6, if 50.4 periods were observed, the value of NSPE is approximately -0.0017 and the approximate average power is $P_T(1+.0017)$ or 0.17% above the true power. This power measurement error is well within the acceptable limit for most power measurements. Figure 6 also reflects that the maximum absolute error is smaller for $C_n = 100$ rather than for $C_n = 127$ where the $\sin(2\pi C/N)$ is approximately unity. This is due to the phase shift angle θ which is 30° for this case. Since NSPE is oscillatory, it would be advantageous to determine the maximum and minimum values for any period between $C=1$ and 255. This approach would give the worst case error for any period ($1 \leq C \leq 255$). The behavior of the minimum worst case as a function of C can be studied for various values of phase angles.

A computer program was developed to determine $NSPE_{max}$ and $NSPE_{min}$ for any period C_n where C_n could vary from 1 to 255. Figure 7 shows the behavior of $NSPE_{max}$ as a function of periods observed for $\theta = \pm 30^{\circ}$ and $N = 512$. For the stated phase angles, $NSPE_{max}$ reaches approximately the same global minimum but in different numbers of periods. This minimization is primarily due to the $\sin(2\pi C/N)$ factor and the phase angle. Figure 8 shows the variation of $NSPE_{min}$ for the same range of C as in Figure 7.

The results of the section reflect the importance of having a matched frequency response for H_V and H_I when the bandwidth of the power meter is comparable to the highest important

harmonic power associated with periodic voltage and current signals. Also, harmonics with large voltage and current magnitudes may contribute very little average power if the phase angle is near $\pm 90^\circ$.

In summary, it was found that sampling the voltage and current and processing the results using a microcomputer as a wattmeter can generate excessive power measurement errors if the observation time is comparable to the period of the input signals or if the number of observation periods approaches half the memory size used to store the samples of voltage or current in the computer.

IV. POWER ERROR ANALYSIS OF A SIMPLE CHOPPER SYSTEM

As pointed out in Section II, power measurement error is strongly affected by the waveform of the instantaneous voltage and current. Hence, in order to understand the behavior of power measurement error, a specific set of waveforms must be investigated. This section of the report will analyze the power measurement error associated with an ideal simple chopper system [7] that controls the power from the source to a load. In this case, the load will be an ideal shunt motor. The duty cycle of the chopper and the motor's back emf have strong influences on the power measurement error.

In order to evaluate the harmonic input and output power content in an electronic chopper or power controller such as employed in an electric vehicle, the steady state instantaneous input/output voltage and current must be known in terms of the system parameters. A simplified schematic for a DC/DC chopper is shown in Figure 9. Power that is delivered to the shunt motor from the DC source is controlled by switch SW that is activated by an electronic system not shown in the model. By varying the on-time with respect to the time of one period, power supplied to the motor can be varied from zero to a maximum value which depends on the system parameters. For the purpose of analysis, it will be assumed that the time constants of the electric motor and the connecting mechanical load are much larger than the time constant of the power controller.

. The resistances R_1, R_2, and R_3 represent the internal resistance of the DC source and input leads; on-resistance of the switch SW; and resistance of the armature of the shunt motor, respectively. Inductance L_3 accounts for the inductance of the armature. Voltages E_1 and E_2 represents the open-circuit voltage of the D.C. source and the back emf of the motor, respectively, while voltages E_3 and E_4 account for the semiconductor offset voltage. Listed in Figure 9 are the numerical

values of the ·system parameters used in the harmonic analysis of the power controller's input and output signals.

Diode D_1 is necessary to allow the current i_2 to continue to flow after SW is turned off; otherwise the induced voltage across L_3 will approach infinity as i_2 decreases instantaneously to zero. This will cause a voltage breakdown in the power controller. The free-wheeling action of the diode and L_3 increases DC component substantially by taking advantage of the energy stored in the inductor..

Typical voltage and current waveforms are shown in Figure 10. The on-time is represented by T_D and the period by T_P. Obviously, T_D can be varied from 0 to T_P and for purpose of analysis, the period is fixed at 0.001 second.

The harmonic structure of the input/output voltage and current will be required in order to study the behavior of the harmonic power content. The on-time and back emf are the two system parameters that can be varied easily in an electric vehicle. The duty cycle, T_D/T_P, is controlled by the vehicle's operator via the power controller while the back emf depends on the magnetic flux and the speed of the motor. Neglecting armature reaction, the net flux will essentially remain constant for a given shunt field current and armature current. Under this condition, the back emf is directly proportional to the speed of the armature.

The amplitude and phase angle of the harmonics contained in e_1, i_1, e_2 and i_2 will vary with duty cycle for a given back emf. Before quantitatively expressing the harmonic behavior as a function of the on-time, a qualitative assessment can be conducted. This approach reinforces the quantitative results. Starting with a 100% duty cycle, the voltages and currents in the system are pure DC assuming the electrical system in Figure 9 has reached a steady-state condition. As the duty cycle is reduced from 100%, the signals become rich in harmonics and this richness grows as the duty cycle

decreases. However, as the duty cycle approaches zero, the instantaneous voltages and currents and corresponding harmonics as well as the DC component approach zero. For a given duty cycle, the harmonic content in the instantaneous voltages and currents decreases as the back emf approaches the input voltage. This is obvious because the back emf bucks the voltage E_1. The instantaneous voltages and currents are therefore very rich in harmonics when the duty cycle is small and the back emf is approaching zero.

Since the power associated with any given harmonic depends on the amplitude of the voltage and current as well as the cosine difference of the phase angles, large harmonic amplitudes that are approximately in quadrature with each other contribute very little to the total average power. If the DC components of the instantaneous voltage and currents are suppressed as shown in Figure 11, very interesting results can be observed. The fundamental input voltage and current as shown by the dotted curves are approximately 180° out of phase. The exact phase relationship will be a function of the cuty cycle, However, the fundamental output voltage and current appear to be in quadrature, thus contributing very little to the total average power. This is primarily due to the inductive filtering action by the armature inductance which takes place via the diode D_1. Qualitatively, the frequency specifications of a wattmeter monitoring the input power of the power controller will be more stringent than for a wattmeter that is monitoring the power output of the same controller.

A. Fourier Analysis of the Signals Associated with the Simple Chopper System

In order to evaluate the harmonic content of e_1, i_1, e_2 and i_2, the system must be in steady state; otherwise the Fourier series analysis is meaningless. A set of equations representing the instantaneous voltages and currents will be

derived based on circuit boundary conditions. The results of such analysis will allow the determination of total average power, harmonic power content via the Fourier series, and power error due to a wattmeter with a finite bandwidth.

The current, i_1, can be expressed in the form

$$i_1 = K_1 + K_2 \exp(-t/T_1) \; ; \; 0 \leq t \leq T_D \tag{24-a}$$

$$i_0 = 0 \qquad\qquad ; \; T_D \leq t \leq T_P \tag{24-b}$$

where K_1 represents the value of i_1 if the switch SW remains closed indefinitely and is equal to $(E_1-E_4-E_2)/(R_1+R_2+R_2)$, $K_2=i_2(0^-)-K_1$, and $T_1=L_3/(R_1+R_2+R_3)$. The current $i_2(0^-)$ is the minimum value of the output current as indicated in Figure 10. During the time interval when SW is closed, $i_1=i_2$, and during the remaining portion of the period when SW is open, i_2 can be expressed as

$$i_2 = K_3 \exp(-(t-T_D)/T_2) \; ; \; T_D \leq t \leq T_P \tag{25}$$

where $K_3=i_1\big|_{t=T_D}$ and $T_2=L_3/R_3$. It is assumed that i_2 never reaches zero before the switch is closed again. This assumption is reasonable since the time constant T_2 is usually much larger than the period T_P. Equations (24-a) and (25) must have the same value at $t=T_D$ and Equation (25) must be equal to $i_2(0^-)$ at $T=T_P$ since the system is assumed to be in a steady state condition. Thus,

$$K_1 + (i_2(0^-)-K_1)\exp(-T_D/T_1) = K_3; \qquad t=T_D \tag{26-a}$$

$$i_2(0^-) = K_3 \exp(-(T_P-T_D)/T_2) \; ; \qquad t=T_P \tag{26-b}$$

From Equations (26-a) and (26-b), $i_2(0^-)$ can be expressed

in terms of K_1, T_D, T_P, T_1 and T_2 as

$$i_2(0^-) = K_1(1-\exp(-T_D/T_1))/(\exp((T_P-T_D)/T_2)-\exp(-T_D/T_1)). \qquad (27)$$

The value of $i_2(0^-)$ at $t=0$ and $t=T_P$ is in agreement with the electrical bounds on the system, namely, $i_2(0^-)=0$ and $i_2(0^-) = K_1 = (E_1-E_4-E_2)/(R_1+R_2+R_3)$, respectively. The instantaneous input and output voltages can be expressed in terms of the respective currents i_1 and i_2

$$e_1 = E_1 - R_1 i_1 \qquad ; \quad 0 \le t \le T_D \qquad (28\text{-}a)$$

$$e_1 = E_1 \qquad ; \quad T_D \le t \le T_P \qquad (28\text{-}b)$$

$$e_2 = E_1 - (R_1+R_2)i_1 \quad ; \quad 0 \le t \le T_D \qquad (28\text{-}c)$$

$$e_2 = -E_3 \qquad ; \quad T_D \le t \le T_P \qquad (28\text{-}d)$$

Equations (25), (26), (27), (28) are the necessary set of equations to determine the total input and output power, voltage and current harmonics, harmonic power content, and power error due to a wattmeter with a finite bandwidth.

The harmonic content associated with the controller's instantaneous input and output signals can be expressed as a set of algebraic equations whose coefficients are a function of the system parameters. The equations are listed below. See the Appendix for the functional relationship between X_1, X_2, Y_1, Y_2, Y_4, Y_5 and the system parameters.

Input Side of the Power Controller

Voltage Terms

$$W_o = E_1 T_D/T_P - R_1 K_1 T_D/T_P - (R_1 T_1 K_2/T_P)(1-\exp(-T_P/T_1)) + E_1(T_P-T_D)/T_P \qquad (29\text{-}a)$$

$$W_1 = -R(K_1 X_1 + K_2 X_2) \tag{29-b}$$

$$W_2 = -R_1(K_1 Y_1 + K_2 Y_2) \tag{29-c}$$

Current Terms

$$W_{oo} = K_1 T_D / T_P + (K_2 T_1 / T_P)(1 - \exp(-T_D / T_1)) \tag{30-a}$$

$$W_3 = K_1 X_1 + K_2 X_2 \tag{30-b}$$

$$W_4 = K_1 Y_1 + K_2 Y_2 \tag{30-c}$$

$$|V_{n_i}| = ((W_1)^2 + (W_2)^2)^{\frac{1}{2}} \text{ and } \underline{/V_{n_i}} = -\tan^{-1}(W_2 / W_1) \tag{31-a}$$

$$|I_{n_i}| = ((W_3)^2 + (W_4)^2)^{\frac{1}{2}} \text{ and } \underline{/I_{n_i}} = -\tan^{-1}(W_4 / W_3) \tag{31-b}$$

Output Side of the Power Controller

Voltage Terms

$$X_o = (E_1 - E_4) T_D / T_P - (R_1 + R_2) K_1 T_D / T_P - ((R_1 + R_2) T_1 K_2 / T_P)(1 - \exp(-T_D T_1)) - E_3 (T_P - T_D) / T_P \tag{32-a}$$

$$Z_1 = (E_1 - E_4) X_1 - (R_1 + R_2)(K_1 X_1 + K_2 X_2) + E_3 X_1 \tag{32-b}$$

$$Z_2 = (E_1 - E_4) Y_1 - (R_1 + R_2)(K_1 Y_1 + K_2 Y_2) + E_3 Y_1 \tag{32-c}$$

Current Terms

$$X_{oo} = K_1 T_D / T_P + (K_2 T_1 / T_P)(1 - \exp(T_D / T_1)) + (K_3 T_2 / T_P)(1 - \exp(-(T_P - T_D) / T_2)) \tag{33-a}$$

$$Z_3 = K_1 X_1 + K_2 X_2 + K_3 Y_4 \tag{33-b}$$

$$Z_4 = K_1 Y_1 + K_2 Y_2 + K_3 Y_5 \tag{33-c}$$

$$|V_{n_o}| = ((Z_1)^2 + (Z_2)^2)^{\frac{1}{2}} \text{ and } \underline{/V_{n_o}} = -\tan^{-1}(Z_2/Z_1) \tag{34-a}$$

$$|I_{n_o}| = ((Z_3)^2 + (Z_4)^2)^{\frac{1}{2}} \text{ and } \underline{/I_{n_o}} = -\tan^{-1}(Z_4/Z_3) \tag{34-b}$$

Equation (31) and (34) were evaluated using a computer. A typical computer printout is shown in Figure 12. The first thirty harmonics of input/output voltage and current were calculated as a function of on-time T_D for a given E_2. For example, the case where $T_D = 0.0001$ second and $E_2 = 25$ volts, the input fundamental voltage and current are for all practical purposes 180° out of phase while the output fundamental voltage and current are 90° out of phase. This is consistent with the previous discussion about the harmonic phase relationship between voltage and current at both the input and output of the power controller. Although the value of the phase angles for the individual voltage and current are dependent on T_D and E_2, the angular difference between either the input voltage and current or output voltage and current remains independent of T_D and E_2, which is 180° and 90° for the input and output, respectively. Results indicate that the amplitude of the harmonics decreases for increasing T_D and E_2 which is consistent with a physical system. The results of this section are needed for the calculation of the harmonic power content at the input and output of the controller.

B. Total and Harmonic Power of a Simple Chopper System

Total average input and output power can be determined from Equations (24), (25), (26), (27), and (28) by multipling e_1 by i_1, and e_2 by i_2, and averaging the results over one period. The results are

$$P_i = E_1 I_{o_1} - (R_1 K_1^2 T_D)/T_P - (2K_1 K_2 T_1 R_1/T_P)(1-\exp(-T_D/T_1))$$
$$- (K_2^2 T_1 R_1/(2T_P))(1-\exp(-2T_D/T_1)) \tag{35}$$

$$P_o = (E_1 - E_4)I_{o_1} - (R_1 + R_2)(K_1^2 T_D/T_P + (2K_1 K_2 T_1/T_P)(1-\exp(-T_D/T_1))$$
$$+ (K_2^2 T_1/(2T_P))(1-\exp(-2D/T_1))) - (E_3 K_3 T_2/T_P)(1-\exp((T_P-T_D)/T_2)) \tag{36}$$

where I_{o_1} represents the DC input current. See the Appendix.

Harmonic distribution of average power can be determined from the knowledge of the magnitude and phase angle of voltage and current. Frequency roll-off due to the first order input transfer functions of a wattmeter can be incorporated very easily into the power equations. The results are

$$P_{i_{APP}} = W_o W_{oo} + (\tfrac{1}{2})\sum_{n=1}^{N_1}(V_{n_i} I_{n_i}\cos(-\tan^{-1}(W_2/W_1)+\tan^{-1}(W_4/W_3)-\tan^{-1}(n\omega_o/\omega_1)$$
$$+\tan^{-1}(kn\omega_o/\omega_1)))/((1+(n\omega_o/\omega_1)^2)(1+(kn\omega_o/\omega_1)^2))^{\frac{1}{2}}) \tag{37}$$

$$P_{o_{APP}} = X_o X_{oo} + (\tfrac{1}{2})\sum_{n=1}^{N_1}(V_{no} I_{no}\cos(-\tan^{-1}(Z_2/Z_1)+\tan^{-1}(Z_4/Z_3)-\tan^{-1}(n\omega_o/\omega_1)$$
$$+\tan^{-1}(kn\omega_o/\omega_1)))/((1+(n\omega_o/\omega_1)^2)(1+(kn\omega_o/\omega_1)^2))^{\frac{1}{2}}) \tag{38}$$

where N_1 represents the highest harmonic of interest. The other terms were defined in Equations 6, 7, 8, and 9. As long as ω_1 and k remain finite, the power calculated from Equations (37) and (38) will be an approximation of the results from Equations (35) and (36) even if $N_1 \to \infty$. This difference is due to suppression of the higher harmonic power terms by the transfer functions H_V and H_I.

A computer program was developed to evaluate Equations (35), (36), (37) and (38) as functions of the back emf E_2

and the on-time T_D. The computer program calculated a running power sum of approximate input/output power (Equations (37) and (38) as a function of N_1, total input/output power Equations (35) and (36), and the power measurement error.

If the transfer functions' corner frequencies are at least 100 times larger than the fundamental frequency of the periodic signals, it can be reasonably assumed that H_V and H_I are essentially unity and do not effect the power measurement. Assuming wide bandwidth transfer functions, the power measurement error will approach zero as the number of harmonics approaches infinity. However, from a practical viewpoint it is better to consider the necessary number of harmonics in order to achieve a certain power measurement error. For analysis purposes, a power error of 0.01 (1%) was chosen. With this power error objective, the desired error can be attained with relatively few harmonics assuming infinite frequency response. As the corner frequency of the transfer functions begins to approach the fundamental frequency of the periodic signals, more harmonics will be required to achieve a power error of 0.01. If the corner frequencies of the transfer functions are set equal to the fundamental frequency, the power error will be so large that it may be impossible to achieve a power error of 0.01 for certain combinations of back emf E_2 and on-time T_D.

The results of power measurement error versus number of harmonics are shown in Figure 13 a-d. The figures are arranged in an array to emphasize the behavior of power measurement error and the required number of harmonics necessary to achieve a specified numerical value of the power measurement error as a function of E_2 and T_D. The parameters k and f_1 which set the corner frequencies of the transfer functions are varied to study the behavior of the power error. The fundamental frequency is 1000 hertz

(f_o = $1/T_p$). If an error of 0.01 cannot be achieved, this is reflected by indicating the actual error when all 30 harmonics are considered. This will occur when f_1 (f_1 = $\omega_1/2\pi$) is comparable to the fundamental frequency of the signal in the power controller. When T_D is equal to T_p, the power measurement error is zero because the power controller's switch is closed continuously and the voltages and currents are pure DC signals. This is shown in the last row of the array.

The input power measurement error for the case of a wideband wattmeter is shown in Figure 13-a. With k=1 and f_1=100f_o, it is obvious that an error 0.01 can be achieved for all combinations of E_2 and T_D shown. It should be noted that the number of harmonics required to attain 0.01 error varies depending on the combination of E_2 and T_D. The most severe case occuring when E_2=25 and T_D=0.0001 second. Moving diagonally across the array, the required number of harmonics decreases for 0.01 error. This is consistent with the electrical model in Figure 9 since the duty cycle of the power controller is increasing and the E_2 is approaching E_1 which is equal to 100 volts.

Reducing the bandwidth of the wattmeter will cause the power measurement error to increase as shown in Figure 13-b. The first column depicts a condition where an error objective could not be attained even when thirty harmonics were considered. The result is due to the frequency roll-off of the transfer functions interacting with the higher harmonics. Again, moving diagonally across the array the 0.01 error can be achieved with less than 30 harmonics.

If the bandwidth of the transfer functions equal the fundamental frequency, the power measurement error increases drastically and exceeds the 0.01 criterion over more than 50% of the array as shown in Figure 13-c. It is obvious that a wattmeter whose bandwidth is equal to the fundamental

frequency would be practically useless, especially for low values of E_2.

The results shown in Figure 13-d are somewhat similar to Figure 13-c except that the corner frequency of the two wattmeter transfer functions are numerically di-ferent. With k=0.5, one corner frequency is twice the other. Power measurement errors are generally lower for k=0.5 which is to be expected since the effect of the transfer functions on the magnitude of the harmonics is less pronounced. However, with k not equal to unity, the phase angles of the transfer functions do not nullify each other according to Equations (37) and (38) and this causes a phase angle error which in turn affects the power measurement error.

The results of this section of the report illustrate that the harmonic power content at the input is more important than that at the power controller's output. The reason is due to the electrical time constant of the shunt motor. In other words, the inductive reactance X_{L_3} is the predominant con-pared to the armature resistance, R_3, at the harmonic fre-quencies. Hence, a wattmeter having a broader bandwidth must monitor the power input to the power controller.

Depending on the back emf of the shunt motor and the bandwidth of the power meter, there were particular cases where a power measurement error of 0.01 was exceeded, even with all 30 harmonics. This occurred for low duty cycles and small back emfs.

V. POWER ERROR ANALYSIS OF A MICROCOMPUTER WATTMETER

In Section II-B a theoretical investigation was per-
formed to determine the power measurement error due to
sampling an input sinusoidal voltage and current. The
results indicate that the Normalized Sampled Power Error,
NSPE, was very large if a portion of a period was sampled
or if the number of periods sampled approached half of the
data memory capacity, $N/2$, devoted to storing the voltage
or current data. A global minimum value for NSPE occurred
between $C = 0$ and $N/2$ with the position of the minimum NSPE
functionally dependent on the phase angle θ.

This section is primarily concerned with programming a
microcomputer as a wattmeter and studying the behavior of the
microcomputer's output error as a function of observed periods
and phase angles. A commercial 16-bit microcomputer with a
12-bit I/O subsystem was programmed to accept voltage data on
two of the 16 differential protected input channels. Input
channels 0 and 1 were chosen in this case. After computations
were completed by the microcomputer, the output channel 1
displayed the results on a digital voltmeter.

In order to be consistent with Section II-B, the micro-
computer's data memory capacity was set at 512 for each chan-
nel with channel 0 acting as the triggering channel. The
triggering was accomplished by having the microcomputer check
channel 0 for positive zero crossing. This permitted the
microcomputer to process the equivalent of the same data in
case the output reading was questionable.

A program flow chart describing the microcomputer
operation as a wattmeter is shown in Figures 14 a-e. There
are essentially three main parts to this program. The first
segment of the program requires the programmer to set the
sampling interval using a five digit number between 00010

and 10000. The microcomputer's internal timing system is such that a five digit number (xxxxx) divided by 46,875 equals sampling interval in seconds. Therefore, the sampling interval can be varied from approximately 213 microseconds to 213 milliseconds. The minimum sampling time interval was chosen to be ten times the time between sampling channels 0 and 1.

Once the sampling time interval has been set and the teletype return carriage key actuated, the microcomputer observes channel 0 and waits until the signal goes through a positive zero crossing. At that point, both input channels 0 and 1 alternately sample their respective input voltage signals, continuing until the data memories are completely filled. In this case, it would be 512 data points for each channel.

The second part of the program multiplies the first datum from each channel and continues this multiplication in a sequential manner. After each multiplication, the result is added to the results of the previous multiplications with this operation continuing until there are 512 terms. The sum is averaged over the number products and scaled to fit the range of the analog output.

The final part of the program directs the microcomputer back to the start position, ready for the calculation for the next sample interval.

A mathematical relationship between the periods observed, C, and the input frequency, f, can be derived if the sampling time interval T_s is specified. The result is

$$C = NfT_s \qquad (39)$$

where N represents the size of the data memory. As previously stated in this section, the sampling time interval T_s is

$$T_s = (xxxxx)/46875 \qquad (40)$$

where $\qquad$ $10 \leq xxxxx \leq 10000$

Combining Equations (39) and (40), the number of periods observed is

$$C = Nf(xxxxx)/46875 \qquad (41)$$

A program following the flow chart in Figures 14 a-e was written and implemented on a commercial microcomputer. With N equal to 512 and sampling time interval capable of being varied from 213 microseconds to 213 milliseconds, the input frequency was set 36.74 hertz. The choice of frequency was based on the fact that small number of periods were to be observed in order to study the behavior pattern of NSPE. This low frequency also permitted the observation of NSPE for periods approaching N/2.

The results of this section of the report are divided into two segments. The first segment deals with the comparison of the calculated NSPE and theoretical NSPE for the same period of observation. The second segment studies the variation of the microcomputer's output as C approaches N/2.

Figures 15 a-e compare the calculated NSPE with the theoretical NSPE for different phase angles. With an input voltage of 5.010 volts for both channels 0 and 1 and a frequency of 36.74 hertz, the correlation between calculated and theoretical NSPE is poor. This lack of correlation between the two normalized sample power error is believed to be due to either a slight input frequency shifting during the observation time or jitter in the sampling time interval. These effects can cause an uncertaintly in the number of periods that are actually observed. The calculation of the theoretical NSPE is based on the numbers in the first column. The calculated NSPE tends to increase with increasing power factor angle which is consistent with the theoretical calculations of NSPE.

Figure 16 shows the microcomputer's output for different observation periods and phase angles. The bottom row marked true power output reading is used for comparison with actual output readings. For periods 265.64 and 269.66 the output readings are reasonably close to the corresponding theoretical output readings. However, at and near period 267.65, the output readings deviate substantially from the theoretical predictions. The differences are so great that the microcomputer would be useless as a wattmeter for periods observed in the vicinity of 267.65. It is noted that there is a slight difference between the period where the errors are excessive and the predicted period of 256 which is half of the data memory size (N=512). This discrepancy amounts to approximately 5% and is believed to be caused by not knowing the absolute value of the input frequency accurately. As a cross check, the behavior of the microcomputer's output was studied in the vicinity two times 267.65 periods and it was experimentally observed at 536.5 periods the output error was excessive; this is consistent with theory. The ratio of 536.5 to 267.65 is 2.007 which is as close to two as experimentally possible.

The results of this section demonstrate that a microcomputer can be used as a wattmeter providing that the periods observed for the computation is larger than several periods but less than half of the data memory size. As the periods observed approaches N/2, the error is so large that the output reading of the microcomputer is meaningless. This is consistent with the theory presented in Section II-B of this report where Equation (23) relates the functional behavior of NSPE and the observed number of periods. In the denominator of Equation (23-a) the sine function, $\sin(2\pi C/N)$, approaches zero as C approaches N/2 causing the power measurement error to be excessive.

Although the above analysis is based on a single
frequency, the results are applicable for the general case
of periodic signals. If superposition of power is assumed,
it is possible for the observation periods of the harmonics
to be near N/2 or multiples of N/2 causing a serious power
measurement error.

VI. CONCLUDING REMARKS

This study establishes the behavior of power measurement errors due to the bandwidth of $H_v(j\omega)$ and $H_I(j\omega)$, the input transfer functions of a power meter, and the sampling of the input voltage and current of a power instrument.

The frequency response of the power meter's input transfer functions affects both the magnitude and phase angle of the corresponding input sinusoidal voltage and current to the instrument. Since average power depends on the product of the magnitude of voltage and current times the cosine of the power phase angle, the effect of the frequency response is to cause both amplitude and phase distortion which affects the magnitude of the input sinusoidal voltage and current, and the power factor angle, respectively. The power measurement error due to $H_v(j\omega)$ and $H_I(j\omega)$ becomes more pronounced as the frequency of the input voltage and current approaches the bandwidth of $H_v(j\omega)$ and $H_I(j\omega)$, and the power factor approaches zero. Assuming that $H_v(j\omega)$ and $H_I(j\omega)$ are first order transfer functions, the power measurement error due to phase distortion can be eliminated if the two transfer functions have identical frequency responses. Reducing the power measurement error by matching the frequency response of $H_v(j\omega)$ and $H_I(j\omega)$ can be extended to higher order transfer functions. The reason this is true is due to the fact that the voltage and current phase error are subtracted when determining the actual phase angle. Of course, there will always be a power measurement error due to the amplitude distortion of $H_v(j\omega)$ and $H_I(j\omega)$, and the behavior of this error will be strongly dependent on the order of the transfer functions.

When the input sinusoidal voltage and current are sampled, a power measurement error can occur if the samples of the input voltage and current are taken over fractions of a period (not equal to a multiple of half periods) or if the total number of periods observed is equal to one-half

the memory size of either the voltage or current data memory.
The behavior of power measurement error with respect to
cycles observed is due, in part, to the cyclic behavior of
the function, $\sin(2\pi C/N)$, which occurs in the demoninator
of the Normalized Sampled Power Error, NSPE (Equation 23-a).
As $C \rightarrow N/2$, the sine function approaches zero causing the
power measurement error to increase. The numerical value of
NSPE is bounded and equal to -1 as $C \rightarrow N/2$ because the
difference between the cosine functions is also approaching
zero causing Equation (23-a) to have an indeterminate form
at $N/2$. It can be shown that the bound of NSPE at $C = N/2$ is
indeed -1 if $N >> 1$.

Although the above power measurement errors are based on
single frequency analysis, the results are applicable to more
complex periodic signals. Unfortunately, in order to express
the results in a closed form, the periodic signals must
first be analyzed using the Fourier series before the har-
monic power content can be determined. Once the harmonic
power analysis is completed, each harmonic power measurement
error can be determined based on the single frequency analysis
with the resultant power measurement error being the sum of
the harmonic power measurement errors. For periodic signals
it would be more expedient to determine the harmonic power
content contained in periodic signals by directly applying
Fourier series analysis and using Parseval's theorem to
determine the harmonic power distribution. This approach
permits the inclusion of amplitude and phase distortion due
to the presence of the transfer functions $H_V(j\omega)$ and $H_I(j\omega)$.

Since the total power measurement error is dependent
on the weighting factor, P_n/P_T, as indicated in the intro-
duction of this report, the harmonic power distribution does
influence the total power measurement error when the waveform
of either the input voltage or current is changed. Therefore
a power measurement error analysis must be performed on a

given set of voltage and current signals. Input and output voltage and current signals of a simple DC/DC chopper system offer one such set of signals for power measurement error analysis.

Using the duty cycle of the DC/DC chopper and back emf of a shunt motor which is the electrical load for the chopper as the independent variables, a power measurement error analysis was performed by computer. The results indicate that the worst case occurs when the duty cycle of the DC/DC chopper and the back emf of the shunt motor are numerically small. As a general rule, the power measurement error decreases as the duty cycle approaches unity and the back emf of the shunt motor approaches the DC/DC chopper supply voltage.

The results also shows that if the shunt motor armature inductance is large with respect to the armature resistance, the output harmonic power content, excluding the DC power component, is small as compared to the input harmonic power content. This is due to the approximate quadrature phase relationship between the nth harmonic output voltage and current which is caused by the dominance of the inductive reactance at the nth harmonic. Hence, for the DC/DC chopper that was analyzed in this report, the bandwidth specifications for the wattmeter that is measuring the power input to the chopper would be more stringent as compared to the wattmeter that is measuring the power output of the chopper. Although not considered in the electrical model in this report, such electrical phenomena as hysteresis and eddy-current losses can be represented by an equivalent resistance in series with the armature resistance. This resistance combination may be sufficiently large as compared to the armature inductance to cause the output harmonic power to become significant.

This study also investigated the feasibility of using a microcomputer as a wattmeter. Since the microcomputer samples the input voltage and current, the average power for sinusoidal input signals as determined by the microcomputer showed a power measurement error due to sampling. The power measurement error became significant when the number of observed periods C was approximately equal to N/2. The normalized sampled power error was substantially smaller when C was much different from N/2.

The advantages of using a microcomputer as a watt-meter is that instantaneous sampled power, peak power, and the instantaneous sampled voltage and current can be stored and retrieved at a convenient time. When not using the micro-computer as a wattmeter, the microcomputer can be assigned other measuring tasks.

The results of this study can be extended in several areas. For example, in the model of the simple DC/DC chopper system, switching was assumed to be ideal with no losses during the opening and closing of switch SW. Switching transients tend to cause the rate of change of signals to be finite, thus decreasing the amplitudes of the high frequency components in the signal. However, if power analysis of a chopper is desired, the switching losses should be considered. This is especially true if the fundamental chopper frequency is increased to a relative high value. If the signals during switching can be represented by straight-line analysis, the switching power loss can be analyzed separately from the power analysis of the model of the DC/DC chopper in this investigation. By combining the results of both power analyses, the behavior of the power measurement error would represent a more realistic chopper system.

The ideal shunt motor that was assumed in this study could be modified to account for armature reaction and

eddy-current and hysteresis losses. The effect would be
a larger output harmonic power content from the chopper
as compared to the results of this investigation.

The behavior of the power measurement error with re-
spect to back emf and duty cycle would be of great interest
if the shunt motor were replaced by a series motor. The
results could be useful in the electrical efficiency study
of an electrical vehicle since most electric vehicles use
a series motor because of its torque characteristic. How-
ever, power analysis would involve a set of nonlinear
equations due to the nonlinear relationship between the
back emf of the series motor and the DC current output
from the chopper.

Although the use of a microcomputer in this study was
restricted to positive zero crossing input signals, a com-
puter program can be devised so that the microcomputer can
accept a more general class of input signals. With such
an arrangement, the output power reading could be auto-
matically up-dated. Also, the microcomputer could store
such quantities as peak voltage, current, and power and
display this information with the appropriate command.

APPENDIX

Fourier Analysis of the Input/Output Voltage and Current of
a Simple DC/DC Chopper System and the Corresponding Input/
Output Total Average Power.

In Section III of this report, a set of algebraic
equations Equations (31) and (34) were presented based on
the Fourier analysis of the instantaneous voltage and current
at the input and output of a simplified DC/DC chopper system.
These equations were derived from the trigonometric form of
the Fourier series and the general form is given by

$$f(t) = a_o + \sum_{n=1}^{\infty} A_n \cos(n\omega_o t + \Psi_n) \tag{A 1-a}$$

$$a_o = (1/T_p) \int_{-T_p/2}^{T_p/2} f(t) dt \tag{A 1-b}$$

$$a_n = (2/T_p) \int_{-T_p/2}^{T_p/2} f(t) \cos n\omega_o t \, dt \tag{A 1-c}$$

$$b_n = (2/T_p) \int_{-T_p/2}^{T_p/2} f(t) \sin n\omega_o t \, dt \tag{A 1-d}$$

$$A_n = \sqrt{a_n^2 + b_n^2} \quad \text{and} \quad \Psi_n = -\tan^{-1}(b_n/a_n) \tag{A 1-e}$$

where $f(t)$ is a periodic function; a_o represents the average
component of $f(t)$; a_n and b_n represent the in-phase and
quadrature component of the nth harmonic, respectively;
A_n and Ψ_n represents the amplitdue and phase angle of the
n^{th} harmonic, respectively. The angular frequency, ω_o, is

equal to $2\pi/T_P$ where T_P is the time of one period.

This appendix will develop the Fourier series for the input and output voltage and current of the DC/DC simple chopper system and the corresponding input/output total average power. For convenience, the chopper's output signals will be analyzed first using Equation (A-1) and the representation of the instantaneous output voltage and current as developed in Section III.

Output Voltage e_2

$$e_2 = E_1 - R_1 i_1 \quad ; \quad 0 \leq t \leq T_D \tag{A 2-a}$$

$$e_2 = -E_3 \quad ; \quad T_D \leq t \leq T_P \tag{A 2-b}$$

$$i_2 = K_1 + K_2 \exp(-t/T_1) \quad ; \quad 0 \leq t \leq T_D \tag{A 2-c}$$

$$i_2 = K_3 \exp(-(t-T_D)/T_2) ; \quad T_D \leq t \leq T_P \tag{A 2-d}$$

$$a_n = (2/T_P) \int_0^{T_D} (E_1 - E_4 - (R_1 + R_2)(K_1 + K_2 \exp(-t/T_1))) \cos(n\omega_o t) dt$$
$$- (2E_3/T_P) \int_{T_D}^{T_P} \cos(n\omega_o T) dt \tag{A 3-a}$$

$$b_n = (2/T_P) \int_0^{T_D} (E_1 - E_4 - (R_1 + R_2)(K_1 + K_2 \exp(-t/T_1))) \sin(n\omega_o t) dt \tag{A 3-b}$$
$$- (2E_3/T_P) \int_{T_D}^{T_P} \sin(n\omega_o t) dt$$

$$a_\Theta = (1/T_P) \int_0^{T_D} (E_1 - E_4 - (R_1 + R_2)(K_1 + K_2 \exp(-t/T_1))) dt - (E_3/T_P) \int_{T_D}^{T_P} dt. \tag{A 3-c}$$

It is convenient to evaluate the following set of integrals because they occur in several places in Equation (A3).

$$X_1 = (2/T_P) \int_0^{T_P} \cos(n\omega_o t)dt = 2\sin(2\pi n T_D/T_P)/(2\pi n) \qquad \text{(A 4-a)}$$

$$X_2 = (2/T_P) \int_0^{T_D} \exp(-t/T_1)\cos(n\omega_o t)dt = (2/((1/T_1)^2+(n\omega_o)^2))$$

$$\qquad \text{(A 4-b)}$$

$$((\exp(-T_D/T_1))((-1/(T_P T_1))\cos(2\pi n T_D/T_P)+(2\pi n/T_P^2)\sin(2\pi n T_D/T_P))$$

$$+ (1/T_P T_1))$$

$$X_3 = (-2/T_P) \int_{T_D}^{T_P} \cos(n\omega_o t)dt = 2\sin(2\pi n T_D/T_P)/(2\pi n) \qquad \text{(A 4-c)}$$

$$X_o = (E_1-E_4)T_D/T_P-(R_1+R_2)K_1 T_D/T_P-((R_1+R_2)T_1 K_2/T_P)(1-\exp(-T_D/T_1))$$

$$\qquad \text{(A 4-d)}$$

$$-\, E_3(T_P-T_D)/T_P$$

$$Y_1 = (2/T_P) \int_0^{T_D} \sin(n\omega_o t)dt = 2(1-\cos(2\pi n T_D/T_P))/(2\pi n) \qquad \text{(A 4-e)}$$

$$Y_2 = (2/T_P) \int_0^{T_D} \exp(-t/T_1)\sin(n\omega_o t)dt =$$

$$(2/((1/T_1)^2+(n\omega_o)^2))((\exp(-T_D/T_1))((-1/(T_P T_1))\sin(2\pi n T_D/T_P) \qquad \text{(A 4-f)}$$

$$- (2\pi n/T_P^2)\cos(2\pi n T_D/T_P)) + 2\pi n/T_P^2)$$

$$Y_3 = (-2/T_P) \int_{T_D}^{T_P} \sin(n\omega_o t) dt = 2(1-\cos(2\pi n T_D/T_P))/(2\pi n) = Y_1. \quad \text{(A 4-g)}$$

Let

$$Z_1 = (E_1-E_4)(X_1) - (R_1+R_2)(K_1X_1+K_2X_2) + E_3X_1 \qquad \text{(A 5-a)}$$

$$Z_2 = (E_1-E_4)(Y_1) - (R_1+R_2)(K_1Y_1+K_2Y_2) + E_3Y_1. \qquad \text{(A 5-b)}$$

The amplitude and phase angle of the nth harmonic output voltage can be expressed in terms of Z_1 and Z_2 as follows:

$$V_{n_o} = ((Z_1)^2+(Z_2)^2)^{\frac{1}{2}} \text{ and } \underline{/V_{n_o}} = -\tan^{-1}(Z_2/Z_1). \qquad \text{(A 6)}$$

Hence the Fourier series for the output voltage is

$$e_2(t) = X_o + \sum_{n=1}^{\infty} V_{n_o} \cos(n\omega_o t - \tan^{-1}(Z_2/Z_1)). \qquad \text{(A 7)}$$

Output Current i_2

$$a_n = (2/T_P) \int_0^{T_D} (K_1+K_2\exp(-t/T_1))\cos(n\,\omega_o t) dt$$

$$+ (2/T_P) \int_{T_D}^{T_P} (K_3\exp(-(t-T_D)/T_2))\cos(n\omega_o t) dt \qquad \text{(A 8-b)}$$

$$b_n = (2/T_P) \int_0^{T_D} (K_1 + K_2 \exp(-t/T_1)) \sin(n\omega_o t) dt$$

$$+ (2/T_P) \int_{T_D}^{T_P} (K_3 \exp(-(t-T_D)/T_2)) \sin(n\omega_o t) dt \tag{A 8-b}$$

$$a_o = (1/T_P) \int_0^{T_D} (K_1 + K_2 \exp(-t/T_1)) dt + (1/T_P) \int_{T_D}^{T_P} (K_3 \exp(-(t-T_D)/T_2)) dt. \tag{A 8-c}$$

Again, it is convenient to evaluate the following set of integrals because they occur in several places in Equation (A 8).

$$Y_4 = ((2\exp(T_D/T_2))/T_P) \int_{T_D}^{T_P} (\exp(-t/T_2)) \cos(n\omega_o t) dt =$$

$$((2\exp(T_D/T_2))/((1/T_2)^2 + (n\omega_o)^2))((-1/(T_P T_2)) \exp(-T_P/T_2)$$

$$- (\exp(-T_D/T_2))((-1/(T_P T_2)) \cos(2\pi n T_D/T_P)$$

$$+ (2\pi n/T_P^2) \sin(2\pi n T_D/T_P)) \tag{A 9-a}$$

$$Y_5 = ((2\exp(T_D/T_2))/T_P) \int_{T_D}^{T_P} \exp(-t/T_2) \sin(n\omega_o t) dt =$$

$$((2\exp(T_D/T_2))/((1/T_2)^2 + (n\omega_o)^2))((-2\pi n/T_P^2) \exp(-T_P/T_2)$$

$$- (\exp(-T_D/T_2))((-1/(T_P T_2)) \sin(2\pi n T_D/T_P)$$

$$- (2\pi n/T_P^2) \cos(2\pi n T_D/T_P))) \tag{A 9-b}$$

$$Y_o = K_1 T_D/T_P + (K_2 T_1/T_P)(1-\exp(-T_D/T_1)) + (K_3 T_2/T_P)(1-\exp(-(T_P-T_D)/T_2)). \quad \text{(A. 9-c)}$$

Let

$$Z_3 = K_1 X_1 + K_2 X_2 + K_3 X_4 \qquad \text{(A 10-a)}$$

$$Z_4 = K_1 Y_1 + K_2 Y_2 + K_3 Y_5. \qquad \text{(A 10-b)}$$

The amplitude and phase angle of the nth harmonic output current can be expressed in terms of Z_3 and Z_4.

$$I_{n_o} = ((Z_3)^2 + (Z_4)^2)^{\frac{1}{2}} \text{ and } \underline{/I_{n_o}} = -\tan^{-1}(Z_4/Z_3). \qquad \text{(A 11)}$$

Hence the Fourier series for the output current is

$$i_2(t) = Y_o + \sum_{n=1}^{\infty} I_{n_o} \cos(n\omega_o t - \tan^{-1}(Z_4/Z_3)). \qquad \text{(A 12)}$$

At the input to the simple DC/DC chopper system, the instantaneous voltage and current is

$$e_1 = E_1 - R_1(K_1 + K_2 \exp(-t/T_1)); \quad 0 \le t \le T_D \qquad \text{(A 13-a)}$$

$$e_1 = E_1 \qquad\qquad ; \quad T_D \le t \le T_P \qquad \text{(A 13-b)}$$

$$i_1 = K_1 + K_2 \exp(-t/T_1) \qquad ; \quad 0 \le t \le T_D \qquad \text{(A 13-c)}$$

$$i_1 = 0 \qquad\qquad\qquad ; \quad T_D \le t \le T_P \qquad \text{(A 13-d)}$$

The in-phase, quadrature, and average Fouries series components for the input voltage are

Input Voltage e_1

$$a_n = (2/T_P) \int_0^{T_D} (E_1 - R_1(K_1 + K_2 \exp(-t/T_1)))\cos(n\omega_o t)dt$$

$$+ (2E_1/T_P) \int_{T_D}^{T_P} \cos(n\omega_o t)dt \tag{A 14-a}$$

$$b_n = (2/T_P) \int_0^{T_D} (E_1 - R_1(K_1 + K_2 \exp(-t/T_1)))\sin(n\omega_o t)dt$$

$$+ (2E_1/T_P) \int_{T_D}^{T_P} \sin(n\omega_o t)dt \tag{A 14-b}$$

$$a_o = (1/T_P) \int_0^{T_D} (E_1 - R_1(K_1 + K_2 \exp(-t/T_1)))dt + (E_1/T_P) \int_{T_D}^{T_P} dt. \tag{A 14-c}$$

Since the mathematical form of Equation (A 14) is similar to Equation (A 3), the amplitude and phase of the nth harmonic is given by

$$W_1 = -R_1(K_1 X_1 + K_2 X_2) \tag{A 15-a}$$

$$W_2 = -R_1(K_1 Y_1 + K_2 Y_2) \tag{A 15-b}$$

$$W_o = E_1 T_D/T_P - R_1 K_1 T_D/T_P - (R_1 T_1 K_2/T_P)(1-\exp(-T_D/T_1)) + E_1(T_P-T_D)/T_P \tag{A 15-c}$$

$$V_{n_i} = ((W_1)^2 + (W_2)^2)^{\frac{1}{2}} \text{ and } \angle V_{n_i} = -\tan^{-1}(W_2/W_1). \tag{A 16}$$

The Fourier series for the input voltage e_1 is

$$e_1 = W_o + \sum_{n=1}^{\infty} V_{n_i} \cos(n\omega_o t - \tan^{-1}(W_2/W_1)) \tag{A 17}$$

Input Current i_1

The in-phase, quadrature, and average Fourier series components for the input voltage are

$$a_n = (2/T_P) \int_0^{T_D} (K_1 + K_2 \exp(-t/T_1)) \cos(n\omega_o t) dt \qquad \text{(A 18-a)}$$

$$b_n = (2/T_P) \int_0^{T_D} (K_1 + K_2 \exp(-t/T_1)) \sin(n\omega_o t) dt \qquad \text{(A 18-b)}$$

$$a_o = (1/T_P) \int_0^{T_D} (K_1 + K_2 \exp(-t/T_1)) dt. \qquad \text{(A 18-c)}$$

Since the mathematical form of Equation (A 18) is similar to Equation (A 8), the amplitude and phase of the nth harmonic are given by

$$W_3 = K_1 X_1 + K_2 X_2 \qquad \text{(A 19-a)}$$

$$W_4 = K_1 Y_1 + K_2 Y_2 \qquad \text{(A 19-b)}$$

$$W_{oo} = K_1 T_D/T_P + (K_2 T_1/T_P)(1 - \exp(-T_D/T_1)) \qquad \text{(A 19-c)}$$

$$I_{n_i} = ((W_3)^2 + (W_4)^2)^{\frac{1}{2}} \quad \text{and} \quad \underline{/I_{n_i}} = -\tan^{-1}(W_4/W_3). \qquad \text{(A 20)}$$

The Fourier series for the input current i_1 is

$$i = W_{oo} + \sum_{n=1}^{\infty} I_{n_i} \cos(n\omega_o t - \tan^{-1}(W_4/W_3)) \qquad \text{(A 21)}$$

In Section III of this report, Equations (35) and (36) represent the total average power input and output of a simple DC/DC chopper system. The total average input and output power can be determined from Equations (24), (25), (26), (27), and (28) by multiplying e_1 by i_1 and e_2 by i_2, respectively; and averaging the results over one period. The instantaneous input and output power is

$$P_i = (E_1 - R_1 i_1) i_1 \quad ; \quad 0 \le t \le T_D \qquad \text{(A 22-a)}$$

$$P_i = 0 \quad ; \quad T_D \le t \le T_P \qquad \text{(A 22-b)}$$

$$P_o = (E_1 - E_4 - (R_1 + R_2) i_1) i_1 \quad ; \quad 0 \le t \le T_D \qquad \text{(A 22-c)}$$

$$P_o = -E_3 i_2 \quad ; \quad T_D \le t \le T_P \qquad \text{(A 22-d)}$$

The average total input and output power is

$$P_i = (E_1/T_P) \int_0^{T_D} i_1 \, dt - (R_1/T_P) \int_0^{T_P} i_1^2 \, dt \qquad \text{(A 23-a)}$$

$$P_o = ((E_1 - E_4)/T_P) \int_0^{T_D} i_1 \, dt - ((R_1 + R_2)/T_P) \int_0^{T_D} i_1^2 \, dt - (E_3/T_P) \int_{T_D}^{T_P} i_2 \, dt, \qquad \text{(A 23-b)}$$

respectively. Evaluating Equation (23) the results are

$$P_i = E_1 I_{o_1} - R_1 K_1^2 T_D/T_P - (2 K_1 K_2 T_1 R_1/T_P)(1 - \exp(-T_D/T_1))$$

$$- (K_2^2 T_1 R_1/(2 T_P))(1 - \exp(-2 T_D/T_1)) \qquad \text{(A 24-a)}$$

$$P_o = (E_1 - E_4) I_{o_1} - (R_1 + R_2)(K_1^2 T_D/T_P + (2 K_1 K_2 T_1/T_P)(1 - \exp(-T_D/T_1))$$

$$+ (K_2^2 T_1/(2 T_P))(1 - \exp(-2 R_D/T_1))) - (E_3 K_3 T_2/T_P)(1 - \exp(-(T_P - T_D)/T_2))$$

$$\text{(A 24-b)}$$

Where I_{o_1} is given by

$$I_{o_1} = (1/T_P) \int_0^{T_D} i_1 dt = K_i T_D/T_P + (K_2 T_1/T_P)(1-\exp(-T_D/T_1)) \qquad (A\ 25)$$

Equations (A 6), (A 7), (A 11), (A 12), (A 16), (A 17), (A 20), (A 21), (A 22), (A 23), (A 24), and (A 25) were programmed on a computer. The program was arranged so that either the behavioral harmonic distribution up to and including the first 30 harmonics of the signals associated with simplifie DC/DC chopper system could be studied as a function of on-time T_D and back emf, E_2, or the power distribution over the same range of harmonics could be studied as a function of on-time and back emf.

DEFINITION OF SYMBOLS

C = number of observed periods

C_n = n^{th} number of observed periods

ΔC = scanning parameter

E_1 = open-circuit voltage of the DC source (volts)

E_2 = shunt motor back emf (volts)

E_3 = semiconductor offset voltage (volts).

E_4 = semiconductor offset voltage (volts)

e_1 = instantaneous chopper input voltage (volts)

e_2 = instantaneous chopper output voltage (volts)

f = frequency (hertz)

f_1 = corner frequency (hertz)

f_o = fundamental frequency (hertz)

H_I = transfer function in the current branch of the wattmeter

H_V = transfer function in the voltage branch of the wattmeter

I_m = amplitude of a sinusoidal current (amperes)

I_n = amplitude of the nth harmonic current (amperes)

I_{n_i} = amplitude of the nth harmonic chopper input current (amperes)

$\underline{/I_{n_i}}$ = phase angle of the nth harmonic chopper input current (degrees)

I_{n_o} = amplitude of the nth harmonic chopper output current (amperes)

$\underline{/I_{n_o}}$ = phase angle of the nth harmonic chopper output current (degrees)

I_o = DC component of current (amperes)

$i_1(t)$ = instantaneous chopper input current (amperes)

$i_2(t)$ = instantaneous chopper output current (amperes)

$i_2(o^-)$ = minimum chopper output current (amperes)

k = ratio of the 3-db frequencies

Δk = deviation of the ratio of the 3-db frequencies

L_3 = shunt motor armature inductance (henrys)

N $\quad$ = data memory size

N_1 $\quad$ = highest harmonic of interest.

NCF = normalized power correction factor

NPE = normalized power error .

NSPE = normalized sampled power error

n $\quad$ = integer

P_{APP} = approximate total average power (watts)

$P_{i_{APP}}$ = approximate total average chopper input power (watts).

$P_{o_{APP}}$ = approximate total average chopper output power (watts)

$p(t)$ = instantaneous power (watts)

$p(nT_s)$ = sampled instantaneous power (watts)

R_1 $\quad$ = equivalent resistance of the DC source and input leads (ohms)

R_2 $\quad$ = on-resistance of switch SW (ohms).

R_3 $\quad$ = shunt motor armature resistance (ohms)

SW $\quad$ = chopper switch.

T_D $\quad$ = on-time of chopper (seconds)

T_o $\quad$ = observation time (seconds)

T_p $\quad$ = fundamental period (seconds)

T_S $\quad$ = sampling time interval (seconds)

T_1 $\quad$ = electrical time constant of chopper system (seconds)

T_2 $\quad$ = electrical time constant of shunt motor (seconds)

V_m $\quad$ = amplitude of a sinusoidal voltage (volts)

V_n $\quad$ = amplitude of the nth harmonic voltage (volts)

V_{n_i} = amplitude of the nth harmonic chopper input voltage (volts)

$\underline{/V_{n_i}}$ = phase angle of the nth harmonic chopper input voltage (degrees)

V_{n_o} = amplitude of the nth harmonic chopper output voltage (volts)

$\underline{/V_{n_o}}$ = phase angle of the nth harmonic chopper input voltage (degrees).

V_o $\quad$ = DC component of voltage (volts)

x = normalized frequency (f/f_1) .

θ = phase angle between sinusoidal voltage and current (degrees)

ϕ_n = phase angle of the nth harmonic current (degrees)

ψ_n = phase angle of the nth harmonic voltage (degrees)

ω = angular frequency (radians/sec.)

ω_1 = corner angular frequency (radians/sec.)

ω_0 = fundamental angular frequency (radians/sec.)

REFERENCES

1. J. E. Maisel: Error Analysis in the Measurement of Average Power of Sinusoidal Signals; Industry Applications Society Annual Meeting; Cleveland, Ohio; September, 1979.

2. R. S. Turgel: Sampling Techniques for Electric Power Measurement; U.S. Department of Commerce, National Bureau of Standards, NBS Technical Note 870; June, 1975.

3. M. S. Roden: Analog and Digital Communications Systems; Prentice-Hall, Inc.; 1979, pp. 43-50.

4. B. P. Lathi: Signals, Systems and Communication; John Wiley and Sons, Inc.; 1965; pp. 76-83.

5. M. Schwartz: Information Transmission, Modulation, and Noise; McGraw-Hill Book Co.; 1970; pp. 38-39.

6. IBID; pp. 47-51.

7. G. V. Lago and D. L. Waidelich: Transients in Electrical Circuits; Ronald Press Co.; 1958; pp. 283-290.
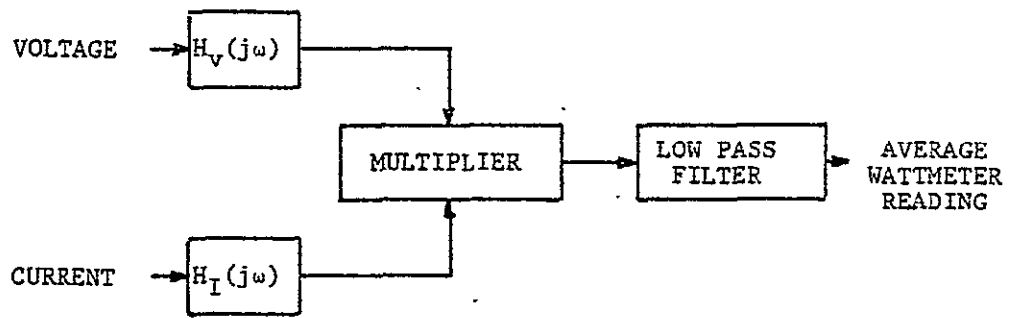
FIGURE 1. General block diagram of á wattmeter.
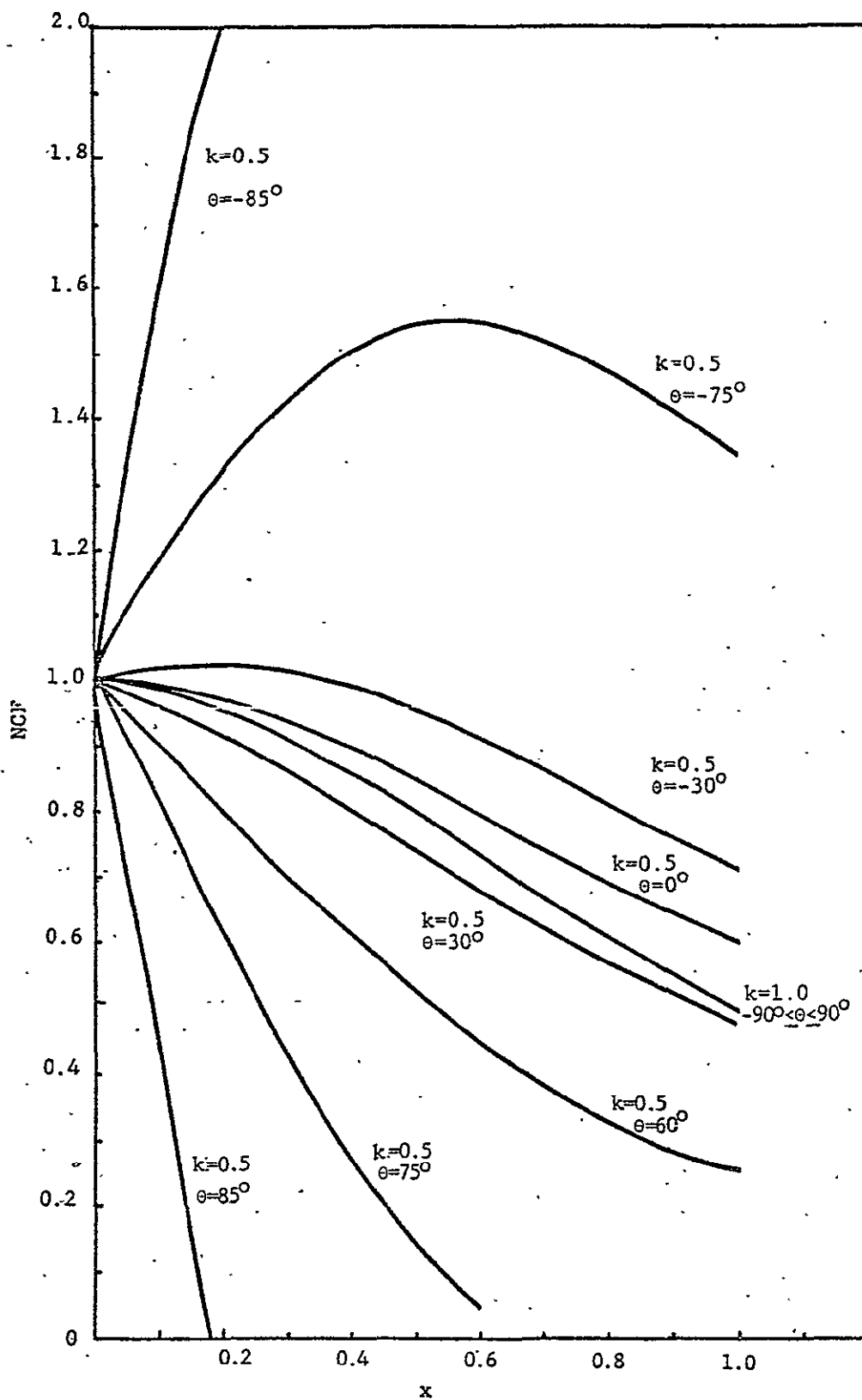
FIGURE 2. Normalized correction factor versus
normalized frequency (k=0.5 and 1.0).
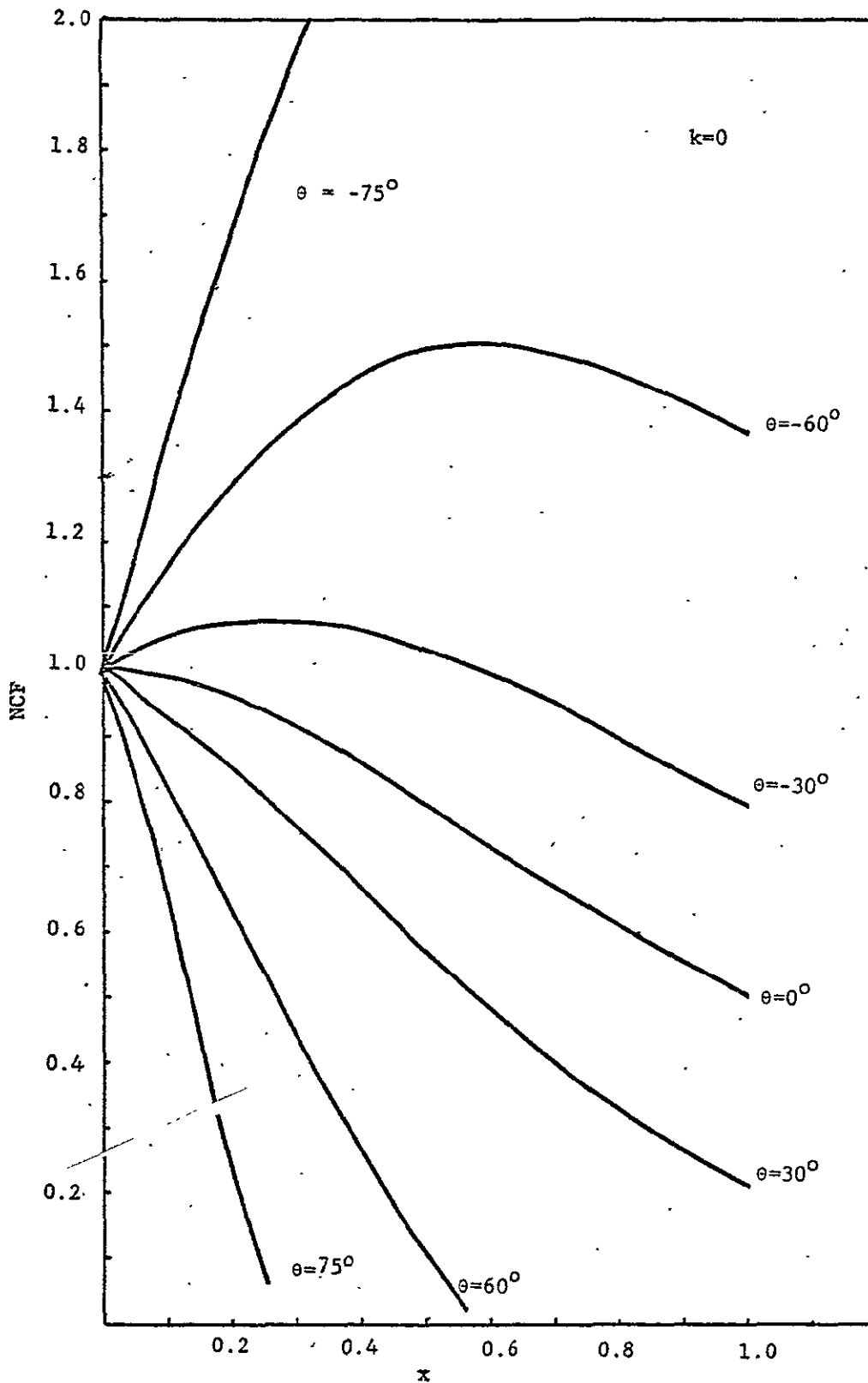
FIGURE 3   Normalized correction factor versus
            normalized frequency (k=0).
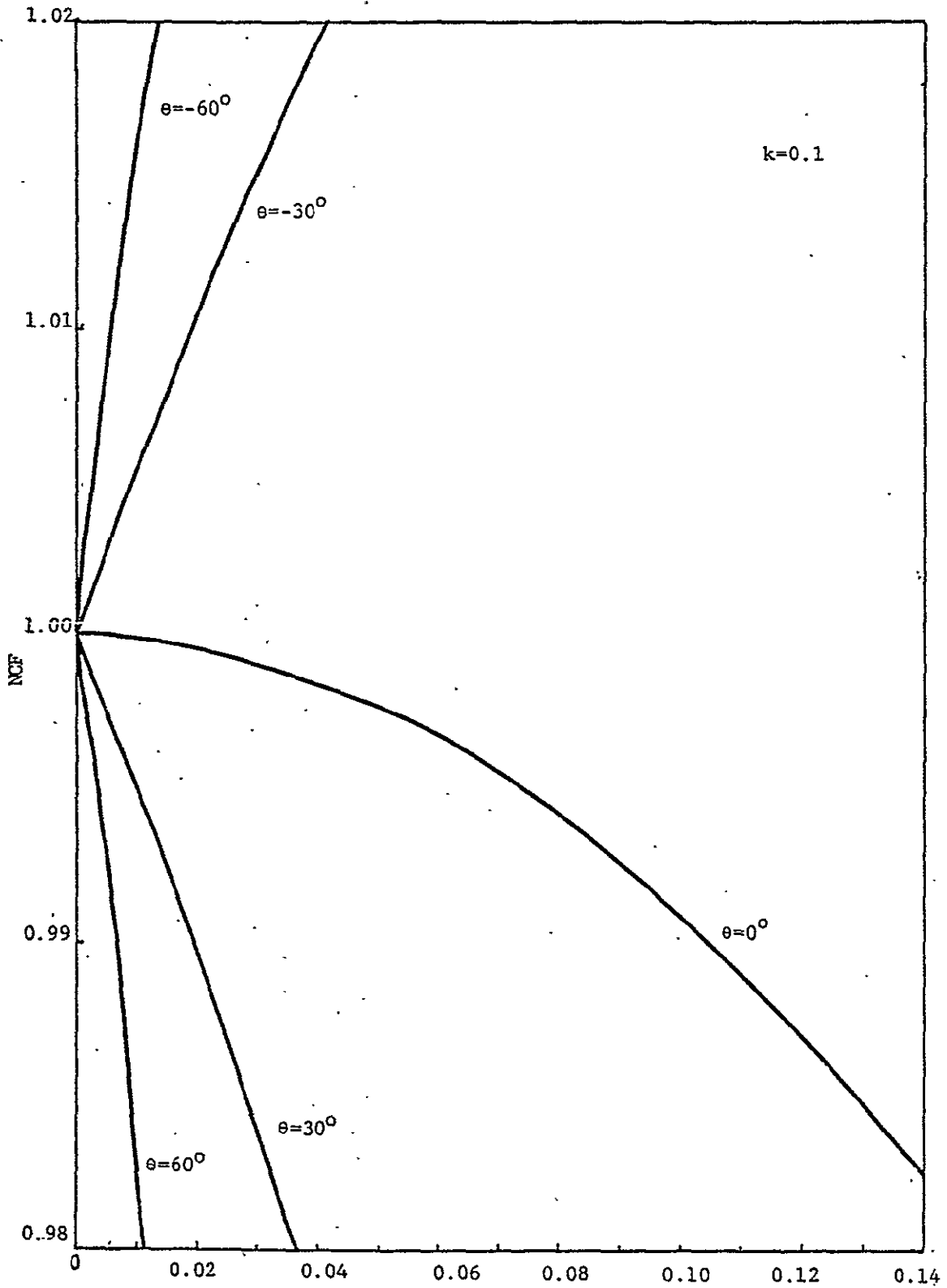
FIGURE 4. Normalized correction factor versus
normalized frequency (k=0.1).
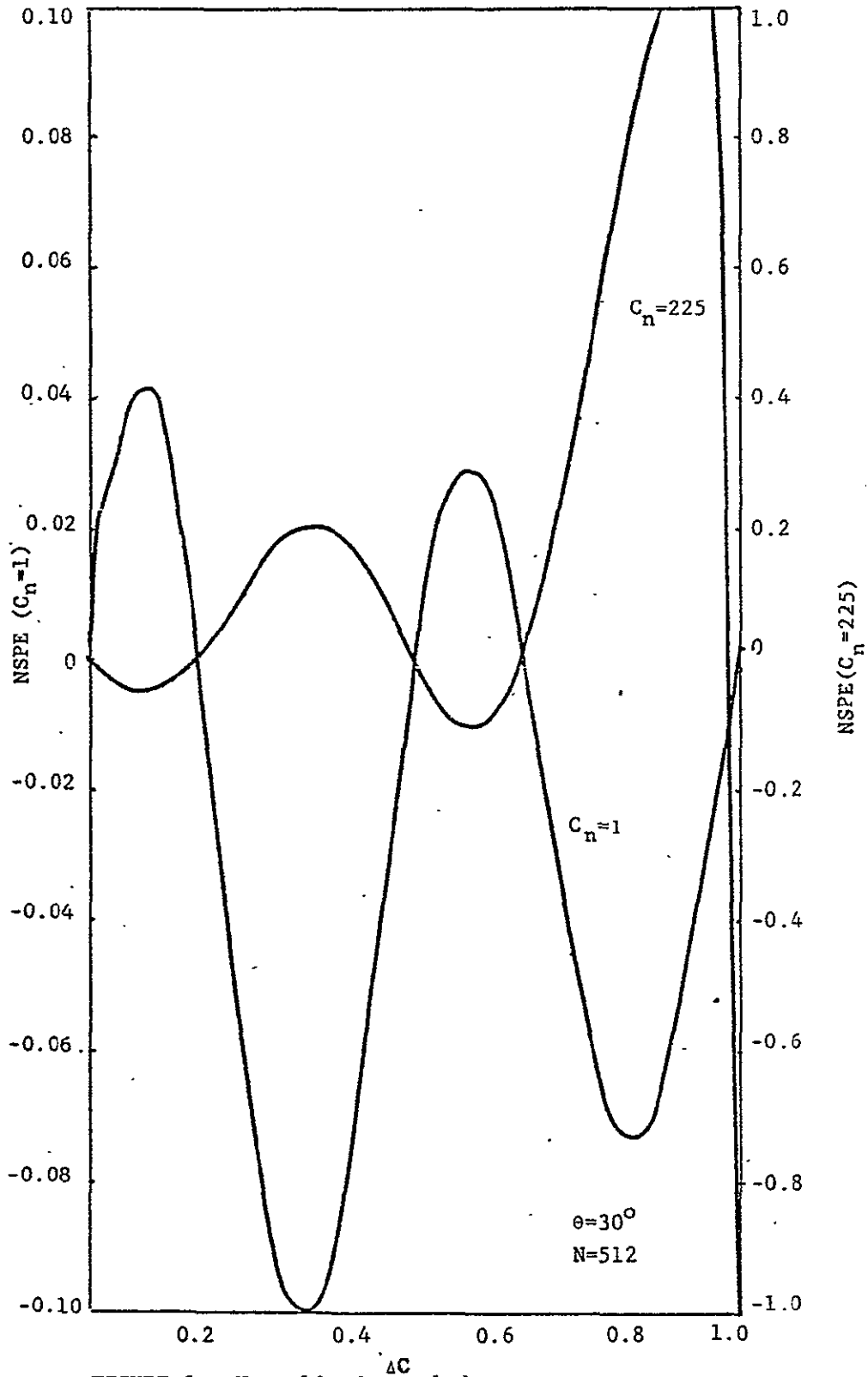
FIGURE 5.   Normalized sampled power error versus
scanning parameter (C_n=1 and 255).
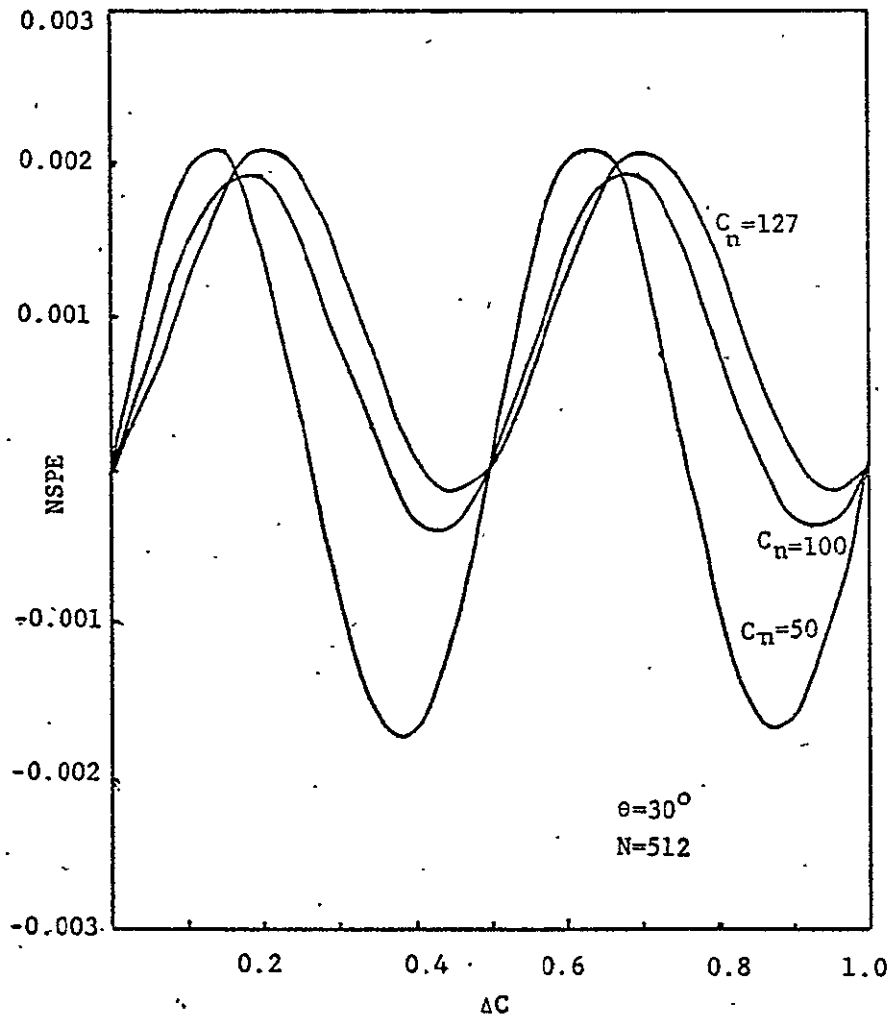
FIGURE 6. Normalized sampled power error versus
scanning parameter (C_n=50, 100., and 127)..
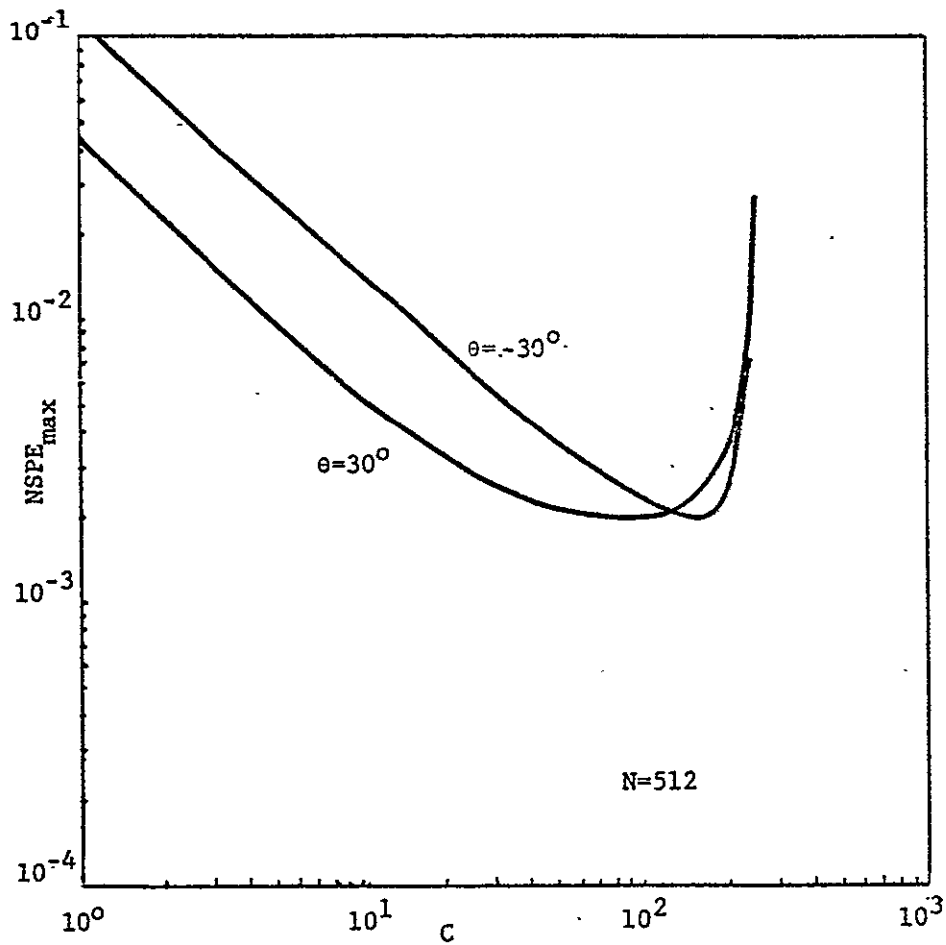
FIGURE 7.   Maximum value of the normalized sampled
            power error versus periods of observation.
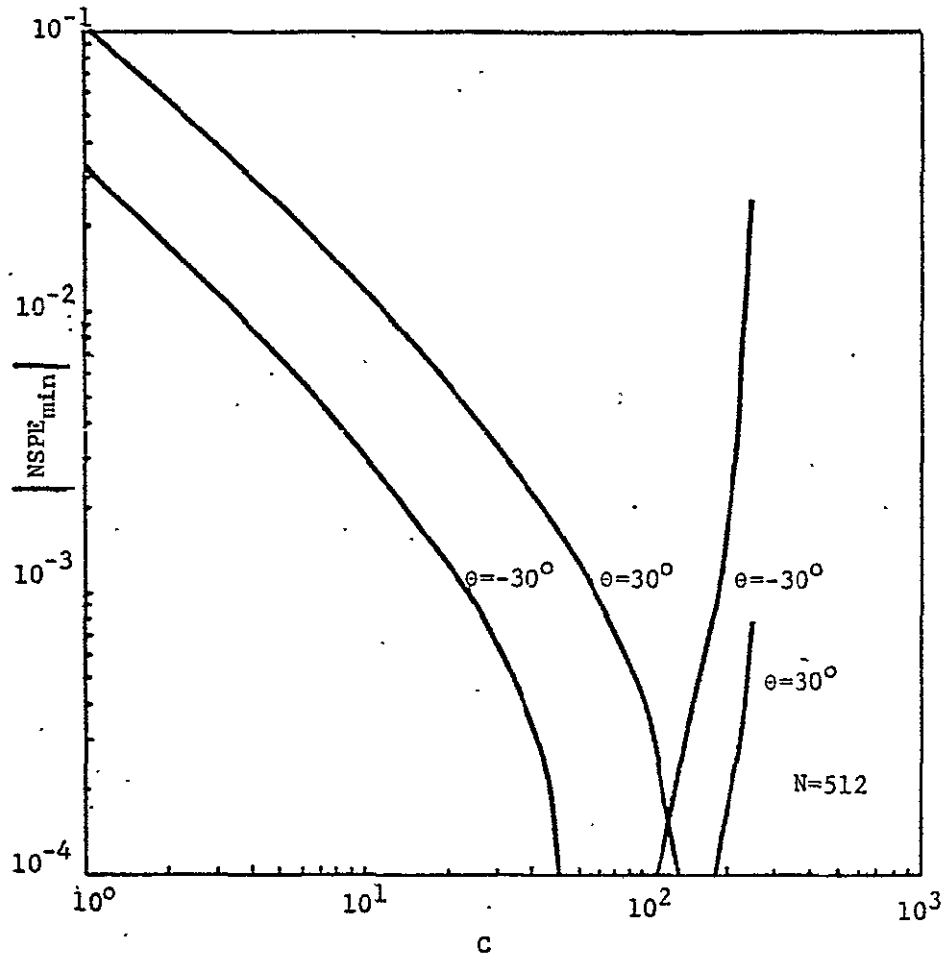
FIGURE 8. The magnitude of the minimum value of
the normalized sampled power error versus
periods of observation.
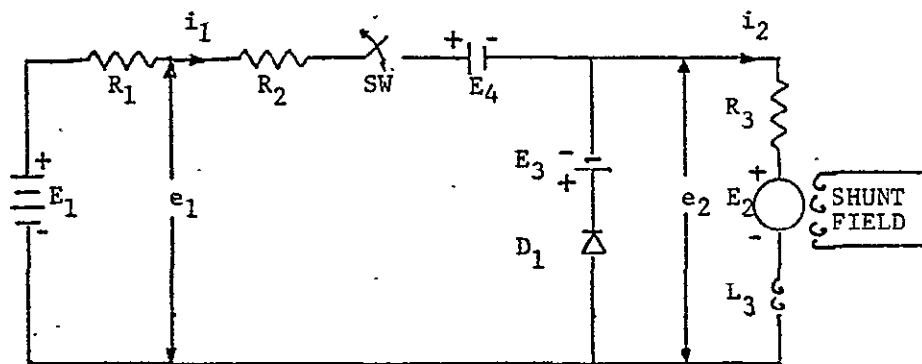
E_1 = 100 volt

E_3 = 1 volt

E_4 = 1 volt

R_1 = 0.05 ohm

R_2 = 0.03 ohm

R_3 = 0.02 ohm

L_3 = 0.0002 henny

FIGURE 9. A schematic for a simple DC/DC chopper.
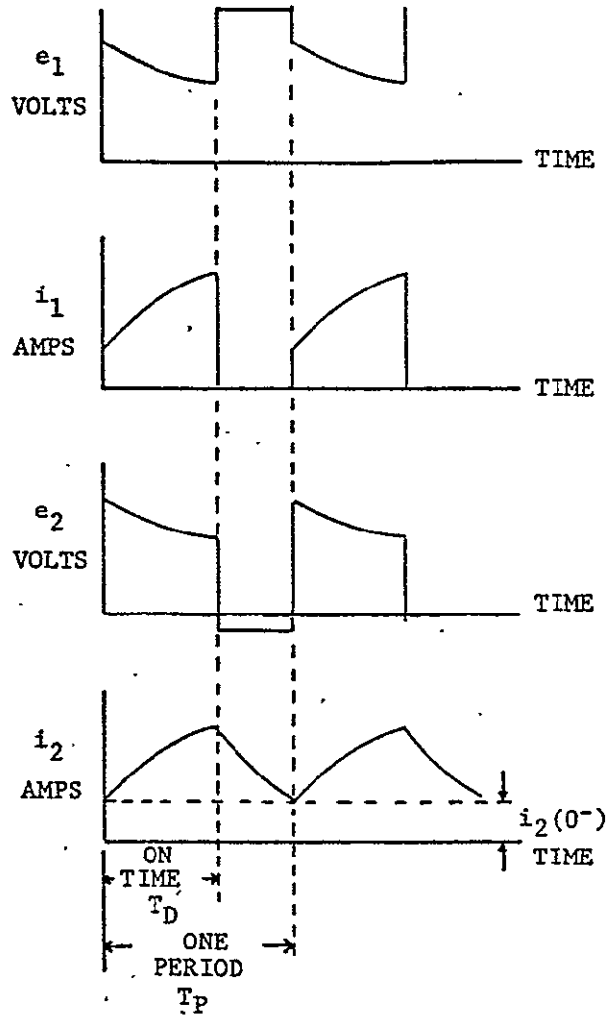
FIGURE 10. Typical operating characteristics for a DC/DC chopper.
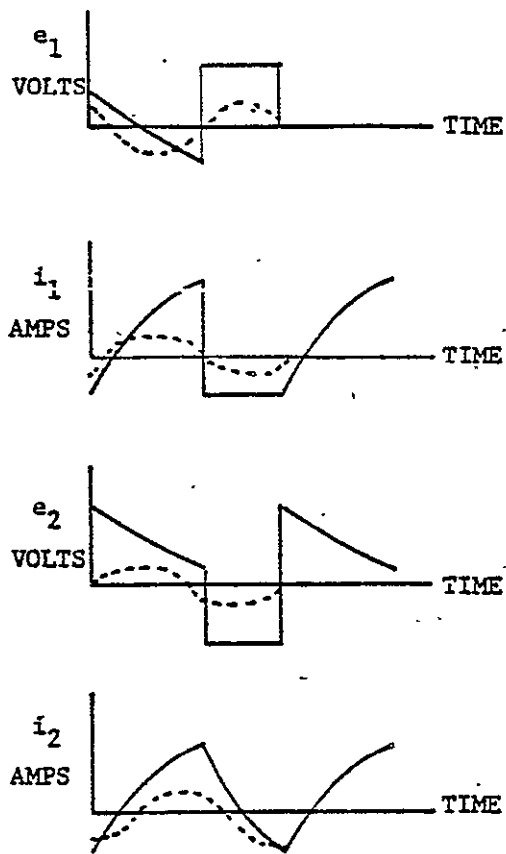
. ---Fundamental component of the periodic signal.

FIGURE 11. Typical operating characteristics for a DC/DC
chopper with the DC component suppressed.

MAISEL
WATTMETER DESIGN
5/17/79

CONSTANTS

R1=   0. 0500
R2=   0. 0300
R3=   0. 0200
E1=   100. 0000
E3=   1. 0000
E4=   1. 0000
T =   0. 0010
T1=   0. 0020
T2=   0. 0100
W1= 62830. 000
K=   1. 0000

E2 =   25. 0000

TD=   0. 0001

I2	P-IN	P-OUT	EFF.	IO1	IO2	
252. 4770	2294. 7000	1820. 5200	0. 7934	26. 4463	237. 7590	

CURRENT/VOLTAGE

| | ****** INPUT ******* | | | | ****** OUTPUT ****** | | | |
N	I MAG	I ANGLE	V MAG	V ANGLE	I MAG	I ANGLE	V MAG	V ANGLE
0. 0000	26. 4463	0. 0000	98. 6777	0. 0000	264. 2150	0. 0000	5. 8848	0. 0000
1. 0000	52. 0225	-18. 2716	2. 6011	-198. 2720	8. 2718	-107. 0370	15. 5107	-17. 9272
2. 0000	49. 4784	-36. 5542	2. 4739	-216. 5540	3. 9338	-125. 4380	14. 7517	-35. 8513
3. 0000	45. 4045	-54. 8615	2. 2702	-234. 8610	2. 4064	-143. 5290	13. 5360	-53. 7668
4. 0000	40. 0374	-73. 2126	2. 0019	-253. 2130	1. 5913	-161. 5190	11. 9344	-71. 6745
5. 0000	33. 6858	-91. 6391	1. 6843	-271. 6390	1. 0708	-179. 4510	10. 0390	-89. 5600
6. 0000	26. 7078	-110. 2020	1. 3354	-290. 2020	0. 7079	-197. 3110	7. 9564	-107. 4070
7. 0000	19. 4883	-129. 0370	0. 9744	-309. 0370	0. 4420	-215. 0560	5. 8014	-125. 1830
8. 0000	12. 4134	-148. 5590	0. 6207	-328. 5580	0. 2459	-232. 5200	3. 6884	-142. 7740
9. 0000	5. 8543	-170. 7610	0. 2927	-350. 7610	0. 1022	-248. 3550	1. 7245	-159. 6290
10. 0000	0. 7569	-269. 5400	0. 0378	-89. 5397	0. 0048	-179. 4390	0. 0605	-89. 5597
11. 0000	4. 7602	-10. 8457	0. 2380	-190. 8460	0. 0685	-111. 4220	1. 4113	-19. 9255
12. 0000	8. 2504	-33. 1380	0. 4125	-213. 1380	0. 1094	-127. 7590	2. 4593	-36. 7675
13. 0000	10. 4736	-52. 7586	0. 5237	-232. 7590	0. 1282	-145. 1770	3. 1242	-54. 3326
14. 0000	11. 4317	-71. 7484	0. 5716	-251. 7480	0. 1299	-162. 3460	3. 4102	-72. 0671
15. 0000	11. 2200	-90. 5466	0. 5610	-270. 5470	0. 1190	-180. 5950	3. 3466	-89. 8531
16. 0000	10. 0069	-109. 3470	0. 5003	-289. 3490	0. 0975	-198. 3340	2. 9839	-107. 6380
17. 0000	8. 0168	-128. 3530	0. 4008	-308. 3530	0. 0749	-215. 9850	2. 3890	-125. 3680
18. 0000	5. 5104	-147. 9950	0. 2755	-327. 9940	0. 0486	-233. 3930	1. 6374	-142. 9260
19. 0000	2. 7677	-170. 2990	0. 1384	-350. 2990	0. 0229	-249. 7070	0. 8170	-159. 7580
20. 0000	0. 3785	-269. 7640	0. 0189	-89. 7641	0. 0012	-179. 7020	0. 0303	-89. 8002
21. 0000	2. 4964	-10. 4964	0. 1248	-190. 4980	0. 0188	-112. 1860	0. 7392	-20. 0207
22. 0000	4. 5021	-32. 8282	0. 2251	-212. 8280	0. 0326	-128. 4940	1. 3414	-36. 8508
23. 0000	5. 9208	-52. 4842	0. 2960	-232. 4840	0. 0410	-145. 3950	1. 7658	-54. 4061
24. 0000	6. 6687	-71. 5040	0. 3334	-251. 5040	0. 0442	-163. 5430	1. 9873	-72. 1324
25. 0000	6. 7316	-90. 3276	0. 3366	-270. 3280	0. 0429	-181. 2870	2. 0080	-89. 9116
26. 0000	6. 1573	-109. 1520	0. 3079	-289. 1520	0. 0377	-199. 0020	1. 8362	-107. 6900
27. 0000	5. 0466	-128. 1740	0. 2523	-308. 1740	0. 0277	-216. 5550	1. 5042	-125. 4160
28. 0000	3. 5413	-147. 8330	0. 1771	-327. 8330	0. 0201	-234. 0500	1. 0539	-142. 9700
29. 0000	1. 8123	-170. 1550	0. 0906	-350. 1550	0. 0098	-250. 3460	0. 5353	-159. 7980
30. 0000	0. 2523	-269. 8360	0. 0126	-89. 8361	0. 0005	-179. 5400	0. 0202	-89. 8902

FIGURE 12.   Typical input/output harmonic distribution for a
simple DC/DC chopper (T_D=0.0001 second and
E_2=25 volts).

$$k = 1 \qquad\qquad f_1 = 10^5 \ \text{Hertz}$$

Power Measurement Error/Minimum Number of Harmonics
Required to Achieve a 0.01 Error (If Possible)

E_2 / T_D	25 VOLTS	50 VOLTS	75 VOLTS	90 VOLTS	95 VOLTS
0.0001 SECOND	0.01 / 16	0.01 / 8	0.01 / 5	0.01 / 2	0.01 / 0
0.0002	0.01 / 13	0.01 / 8	0.01 / 3	0.01 / 2	0.01 / 0
0.0003	0.01 / 12	0.01 / 7	0.01 / 2	0.01 / 1	0.01 / 0
0.0004	0.01 / 11	0.01 / 6	0.01 / 2	0.01 / 1	0.01 / 0
0.0005	0.01 / 9	0.01 / 5	0.01 / 2	0.01 / 1	0.01 / 0
0.0006	0.01 / 9	0.01 / 5	0.01 / 2	0.01 / 1	0.01 / 0
0.0007	0.01 / 8	0.01 / 4	0.01 / 2	0.01 / 1	0.01 / 0
0.0008	0.01 / 7	0.01 / 3	0.01 / 2	0.01 / 0	0.01 / 0
0.0009	0.01 / 6	0.01 / 4	0.01 / 2	0.01 / 0	0.01 / 0
0.0010	0.00 / 0	0.00 / 0	0.00 / 0	0.00 / 0	0.00 / 0

FIGURE 13-a. Input power measurement error versus number of harmonics.

$$k = \underline{\quad 1 \quad} \qquad f_1 = \underline{10^4 \text{ Hertz}}$$

Power Measurement Error/Minimum Number of Harmonics
Required to Achieve a 0.01 Error (If Possible)

T_D \ E_2	25 VOLTS	50 VOLTS	75 VOLTS	90 VOLTS	95 VOLTS
0.0001 SECOND	0.02* / 30	0.02* / 30	0.01 / 6	0.01 / 2	0.01 / 0
0.0002	0.02* / 30	0.01* / 30	0.01 / 4	0.01 / 2	0.01 / 0
0.0003	0.02* / 30	0.01* / 30	0.01 / 3	0.01 / 1	0.01 / 0
0.0004	0.02* / 30	0.01 / 13	0.01 / 3	0.01 / 1	0.01 / 0
0.0005	0.01* / 30	0.01 / 9	0.01 / 3	0.01 / 1	0.01 / 0
0.0006	0.01* / 30	0.01 / 6	0.01 / 2	0.01 / 1	0.01 / 0
0.0007	0.01* / 30	0.01 / 5	0.01 / 2	0.01 / 1	0.01 / 0
0.0008	0.01* / 30	0.01 / 4	0.01 / 2	0.01 / 0	0.01 / 0
0.0009	0.01* / 30	0.01 / 5	0.01 / 2	0.01 / 0	0.01 / 0
0.0010	0.00 / 0	0.00 / 0	0.00 / 0	0.00 / 0	0.00 / 0

* Minimum error achieved by the first 30 harmonics.

FIGURE 13-b. Input power measurement error versus number of harmonics.

k= 1 $\qquad$ $f_1 = 10^3$ Hertz

Power Measurement Error/Minimum Number of Harmonics
Required to Achieve a 0.01 Error (If Possible)

E_2 / T_D	25 VOLTS	50 VOLTS	75 VOLTS	90 VOLTS	95 VOLTS
0.0001 SECOND	0.11* / 30	0.07* / 30	0.03* / 30	0.01* / 30	0.01 / 0
0.0002	0.15* / 30	0.09* / 30	0.04* / 30	0.01* / 30	0.01 / 0
0.0003	0.15* / 30	0.09* / 30	0.04* / 30	0.01* / 30	0.01 / 0
0.0004	0.14* / 30	0.08* / 30	0.04* / 30	0.01* / 30	0.01 / 0
0.0005	0.13* / 30	0.08* / 30	0.03* / 30	0.01* / 30	0.01 / 0
0.0006	0.12* / 30	0.07* / 30	0.03* / 30	0.01 / 3	0.01 / 0
0.0007	0.10* / 30	0.06* / 30	0.02* / 30	0.01 / 1	0.01 / 0
0.0008	0.08* / 30	0.04* / 30	0.02* / 30	0.01 / 0	0.01 / 0
0.0009	0.05* / 30	0.03* / 30	0.01* / 30	0.01 / 0	0.01 / 0
0.0010	0.00 / 0	0.00 / 0	0.00 / 0	0.00 / 0	0.00 / 0

* Minimum error achieved by the first 30 harmonics.

FIGURE 13-c. Input power measurement error versus number of harmonics.

$$k = \underline{0.5} \qquad f_1 = \underline{10^3 \text{ Hertz}}$$

Power Measurement Error/Minimum Number of Harmonics
Required to Achieve a 0.01 Error (If Possible)

T_D \ E_2	25 VOLTS	50 VOLTS	75 VOLTS	90 VOLTS	95 VOLTS
0.0001 SECOND	0.10* / 30	0.07* / 30	0.03* / 30	0.01* / 30	0.01 / 0
0.0002	0.13* / 30	0.08* / 30	0.04* / 30	0.01* / 30	0.01 / 0
0.0003	0.13* / 30	0.08* / 30	0.03* / 30	0.01* / 30	0.01 / 0
0.0004	0.12* / 30	0.07* / 30	0.03* / 30	0.01* / 30	0.01 / 0
0.0005	0.11* / 30	0.06* / 30	0.03* / 30	0.01 / 3	0.01 / 0
0.0006	0.10* / 30	0.06* / 30	0.02* / 30	0.01 / 1	0.01 / 0
0.0007	0.08* / 30	0.05* / 30	0.02* / 30	0.01 / 1	0.01 / 0
0.0008	0.07* / 30	0.04* / 30	0.02* / 30	0.01 / 0	0.01 / 0
0.0009	0.04* / 30	0.02* / 30	0.01* / 30	0.01 / 0	0.01 / 0
0.0010	0.00 / 0	0.00 / 0	0.00 / 0	0.00 / 0	0.00 / 0

* Minimum error achieved by the first 30 harmonics.

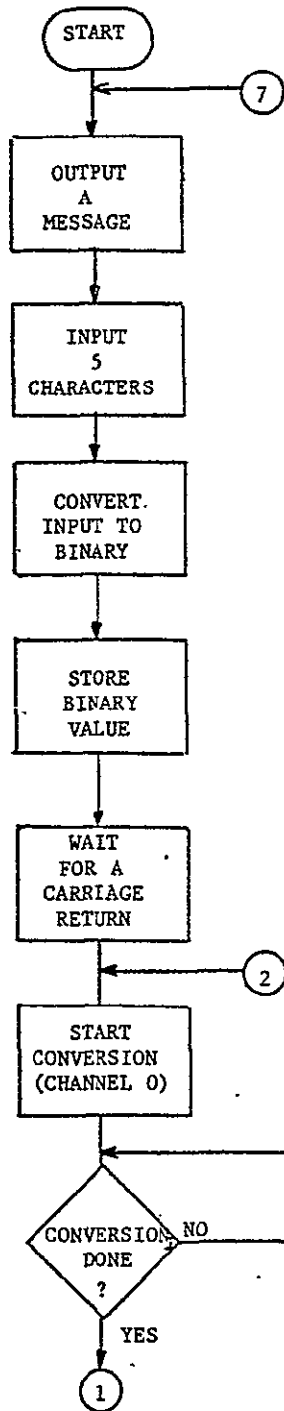FIGURE 13-d. Input power measurement error versus number of harmonics.

FIGURE 14-a. Flow chart for a microcomputer wattmeter.
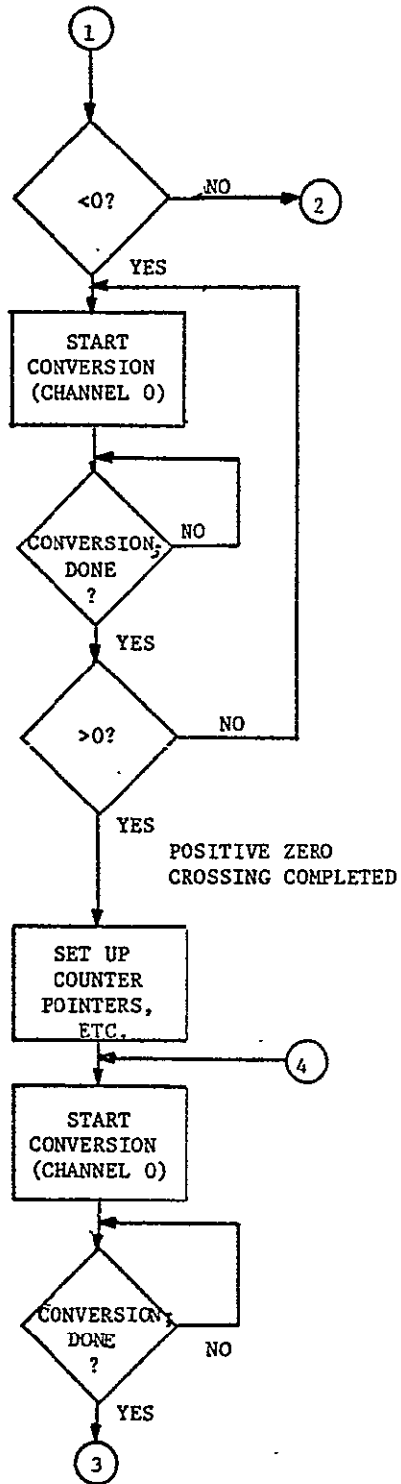
FIGURE 14-b.   Flow chart for a microcomputer
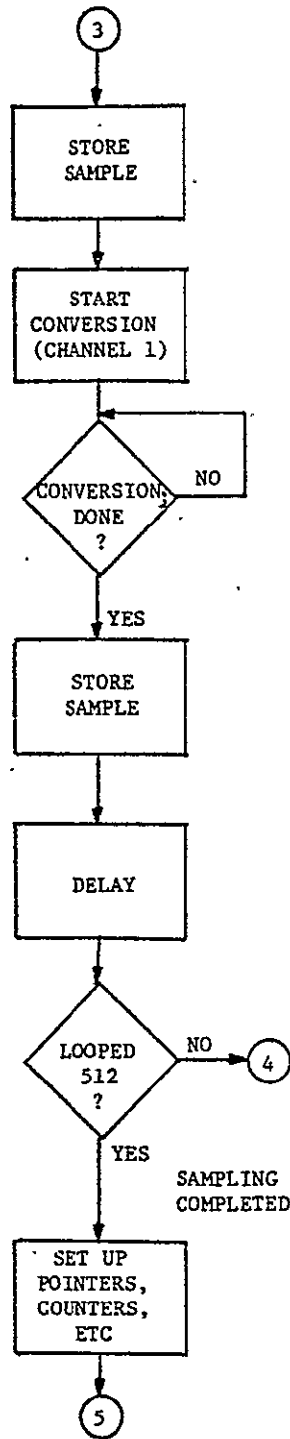wattmeter (continued).

FIGURE 14-c. Flow chart for a microcomputer
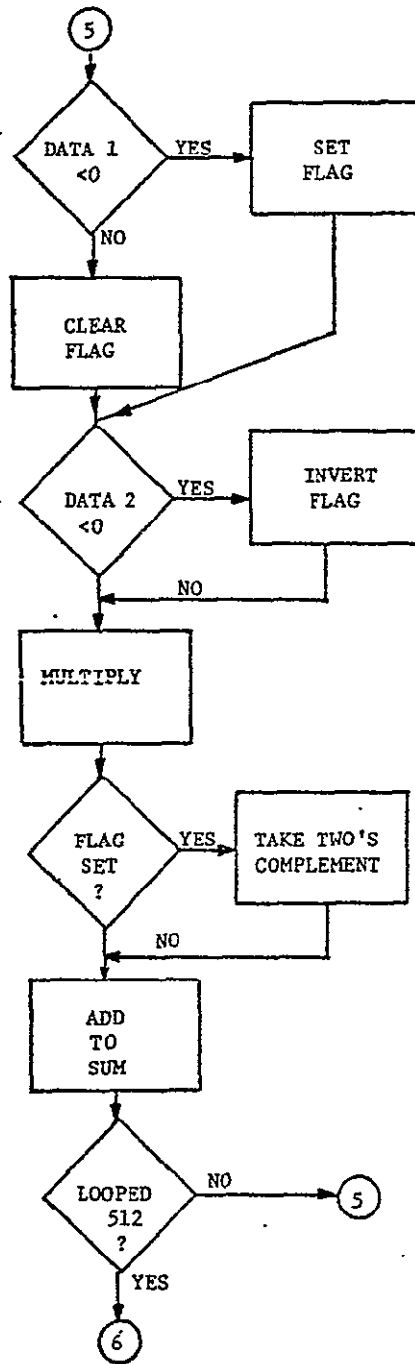   wattmeter (continued).

FIGURE 14-d. Flow chart for a microcomputer wattmeter (continued).
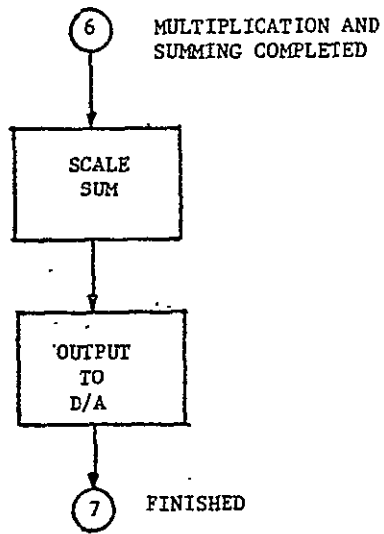
FIGURE 14-e. Flow chart for a microcomputer
wattmeter (continued).

Phase Shift = 0 Degrees
Input Voltage to Channel 0 = 5.010 Volts
Input Voltage to Channel 1 = 5.010 Volts
Frequency of Input Signals = 36.74 Hertz

PERIODS OBSERVED	OUTPUT READING OF MICROCOMPUTER (WATTS)	NSPE	
		MICROCOMPUTER	THEORETICAL
4.01	25.234	-0.0053	0.0025
4.41	25.238	-0.0055	-0.0157
4.81	25.240	-0.0056	-0.0096
5.22	24.847	0.0101	0.0075
5.62	24.904	0.0078	0.0150
6.02	25.429	0.0131	0.0033
6.42	25.142	0.0017	-0.0100
6.82	24.794	0.0122	-0.0074
7.22	25.042	0.0023	-0.0059
7.62	25.190	-0.0036	0.0113
8.02	25.281	-0.0072	0.0025

FIGURE 15-a. Microcomputer output, microcomputer NSPE, and theoretical NSPE versus periods observed.

Phase Shift = 30 Degrees
Input Voltage to Channel 0 = 5.010 Volts
Input Voltage to Channel 1 = 5.010 Volts
Frequency of Input Signals = 36.74 Hertz

PERIODS OBSERVED	OUTPUT READING OF MICROCOMPUTER (WATTS)	NSPE	
		MICROCOMPUTER	THEORETICAL
4.01	22.153	-0.0191	0.0025
4.41	22.013	-0.0127	-0.0222
4.81	21.712	0.0012	-0.0265
5.22	21.624	0.0052	-0.0092
5.62	21.816	-0.0036	0.0079
6.02	22.251	-0.0236	0.0032
6.42	21.817	-0.0037	-0.0138
6.82	21.472	0.0122	-0.0188
7.22	21.959	-0.0102	-0.0061
7.62	22.013	-0.0127	0.0062
8.02	22.006	-0.0124	0.0024

FIGURE 15-b. Microcomputer output, microcomputer NSPE, and theoretical NSPE versus periods observed.

Phase Shift = -30 Degrees
Input Voltage to Channel 0 = 5.010 Volts
Input Voltage to Channel 1 = 5.010 Volts
Frequency of Input Signals = 36.74 Hertz

PERIODS OBSERVED	OUTPUT READING OF MICROCOMPUTER (WATTS)	NSPE	
		MICROCOMPUTER	THEORETICAL
4.01	21.718	0.0009	0.0025
4.41	21.914	-0.0081	0.0092
4.81	22.103	-0.0168	0.0072
5.22	21.578	0.0073	0.0242
5.62	21.424	0.0144	0.0221
6.02	22.009	-0.0125	0.0034
6.42	21.817	-0.0037	-0.0062
6.82	21.666	0.0033	0.0041
7.22	21.575	0.0075	0.0179
7.62	21.717	0.0009	0.0163
8.02	21.959	-0.0102	0.0025

FIGURE 15-c. Microcomputer output, microcomputer NSPE, and theoretical NSPE versus periods observed.

Phase Shift = +60 Degrees
Input Voltage to Channel 0 = 5.010 Volts
Input Voltage to Channel 1 = 5.010 Volts
Frequency of Input Signals = 36.74 Hertz

PERIODS OBSERVED	OUTPUT READING OF MICROCOMPUTER (WATTS)	NSPE	
		MICROCOMPUTER	THEORETICAL
4.01	13.176	-0.0499	0.0024
4.41	12.840	-0.0231	-0.0351
4.81	12.542	0.0006	-0.0602
5.22	12.737	-0.0149	-0.0427
5.62	12.987	-0.0348	-0.0062
6.02	13.124	-0.0457	0.0030
6.42	12.741	-0.0152	-0.0213
6.82	12.542	0.0006	-0.0416
7.22	13.127	-0.0460	-0.0301
7.62	13.036	-0.0387	-0.0039
8.02	12.883	-0.0265	-0.0024

FIGURE 15-d. Microcomputer output, microcomputer NSPE, and theoretical NSPE versus periods observed.

Phase Shift = -60 Degrees
Input Voltage to Channel 0 = 5.010 Volts
Input Voltage to Channel 1 = 5.010 Volts
Frequency of Input Signals = 36.74 Hertz

PERIODS OBSERVED	OUTPUT READING OF MICROCOMPUTER (WATTS)	NSPE	
		MICROCOMPUTER	THEORETICAL
4.01	12.497	0.0042	0.0025
4.41	12.738	-0.0150	0.0037
4.81	13.128	-0.0461	0.0409
5.22	12.597	-0.0037	0.0576
5.62	12.246	0.0242	0.0362
6.02	12.790	-0.0191	0.0036
6.42	12.789	-0.0190	0.0014
6.82	12.687	-0.0109	0.0269
7.22	12.450	0.0080	0.0420
7.62	12.493	0.0045	0.0265
8.02	12.884	-0.0266	0.0026

FIGURE 15-e. Microcomputer output, microcomputer NSPE, and theoretical NSPE versus periods observed.

Input Voltage to Channel 0 = 5.010 Volts
Input Voltage to Channel 1 = 5.010 Volts
Frequency of Input Signals = 36.74 Hertz

PERIODS OBSERVED	OUTPUT READING OF MICROCOMPUTER (WATTS)		
	$\theta = 0^o$	$\theta = 30^o/\theta = -30^o$	$\theta = 60^o/\theta = -60^o$
265.64	24.744	23.424/21.422	14.986/10.929
266.04	26.218	22.156/21.866	13.372/12.499
266.45	24.262	21.039/19.181	13.329/10.977
266.85	21.331.	22.788/17.129	15.957 / 7.416
267.25	22.751	29.287/21.137	22.205 / 4.689
267.65	17.475	1.768/10.782	-8.744/19.176
268.05	24.701	25.377/25.919	14.347/13.768
268.45	27.927	21.235/25.774	10.348/16.887
268.85	26.504	20.107/22.884	10.343/15.277
269.25	24.361	21.426/21.234	12.296/12.744
269.66	24.552	22.502/21.911	13.329/12.492
TRUE POWER READING	25.10	21.74/21.74	12.55/12.55

FIGURE 16. Microcomputer output versus the periods observed for different phase angles.